MARCH 2025 • VOLUME 96 • NUMBER 3, SECTION II, SUPPLEMENT

Aerospace Medicine and Human Performance

THE OFFICIAL JOURNAL OF THE AEROSPACE MEDICAL ASSOCIATION

Risk vs. Benefit Analysis of Ultraviolet-C Advanced Aircraft Disinfection

Aerospace Medicine and Human Performance

MARCH 2025 VOLUME 96 NUMBER 3, SECTION II, SUPPLEMENT [ISSN 2375-6314 (print); ISSN 2375-6322 (online)]

This journal, representing the members of the Aerospace Medical Association, is published for those interested in aerospace medicine and human performance. It is devoted to serving and supporting all who explore, travel, work, or live in hazardous environments ranging from beneath the sea to the outermost reaches of space.

AEROSPACE MEDICAL ASSOCIATION is an organization devoted to charitable, educational, and scientific purposes. The Association was founded when the rapid expansion of aviation made evident the need for physicians with specialized knowledge of the flight environment. Since then, physicians have been joined in this Association by professionals from many fields and from many countries, all linked by a common interest in the health and safety of those who venture into challenging environments.

AEROSPACE MEDICINE AND HUMAN PERFORMANCE, formerly *Aviation, Space, and Environmental Medicine*, is published monthly by the Aerospace Medical Association, a non-profit charitable, educational, and scientific organization of physicians, physiologists, psychologists, nurses, human factors and human performance specialists, engineers, and others working to solve the problems of human existence in threatening environments on or beneath the Earth or the sea, in the air, or in outer space. The original scientific articles in this journal provide the latest available information on investigations into such areas as changes in ambient pressure, motion sickness, increased or decreased gravitational forces, thermal stresses, vision, fatigue, circadian rhythms, psychological stress, artificial environments, predictors of success, health maintenance, human factors engineering, clinical care, and others. This journal also publishes notes on scientific news and technical items of interest to the general reader, and provides teaching material and reviews for health care professionals.

MEMBERSHIP—The Aerospace Medical Association welcomes members interested in aerospace medicine and human performance. Membership applications may be obtained online at www.asma.org or from the Aerospace Medical Association's headquarters at 320 S. Henry Street, Alexandria, VA 22314, or phone the Membership Department at (703) 739-2240; skildall@asma.org.

SUBSCRIPTIONS—*Aerospace Medicine and Human Performance* is provided to all members of the Aerospace Medical Association (online; a print subscription may be purchased separately). Subscriptions and changes of address should be sent to the Subscription Department, *Aerospace Medicine and Human Performance*, 320 S. Henry Street, Alexandria, VA 22314, at least 90 days in advance of change. Institutional Subscription Rates (Online): U.S.-$348, Canada-$348, Other countries-$348 (includes air delivery); Agent Disc.-$20. Individual Subscription Rates (Online): U.S.-$268, Canada-$268, Other countries-$268 (includes air delivery). Single copies and back issues: $30+P/H ($7.50 U.S./$25 International Air). NOTE TO INTERNATIONAL SUBSCRIBERS: Please add $50 for bank handling charges on checks not drawn on U.S. banks.

ADVERTISING—Contracts, Insertion Orders, and Ad Materials (except Inserts): Aerospace Medicine and Human Performance, c/o Kris Herlitz, The Herlitz Company, 108 Montgomery St., Ste. 205, Rhinebeck, NY 12572; Phone: 845-243-2906; kris@herlitz.com. Copy deadline: 10th of second month before date of issue. Inserts: *Aerospace Medicine and Human Performance*, KnowledgeWorks Global, Ltd., 450 Fame Ave., Hanover, PA 17331.

Aerospace Medicine and Human Performance [ISSN 2375-6314 (print); ISSN 2375-6322 (online)], is published monthly by the Aerospace Medical Association, 320 S. Henry St., Alexandria, VA 22314-3579. Periodicals postage paid at Alexandria, VA, and at additional mailing offices. POSTMASTER: Send address changes to *Aerospace Medicine and Human Performance,* 320 S. Henry St., Alexandria, VA 22314-3579. Phone (703) 739-2240. Printed in U.S.A. CPC Int'l Pub Mail #0551775.

Aerospace Medicine and Human Performance

MARCH 2025 VOLUME 96 NUMBER 3, SECTION II, SUPPLEMENT

Risk vs. Benefit Analysis of Ultraviolet-C Advanced Aircraft Disinfection

80% of In-Flight Disease Transmission is Preventable—Here's How AeroClenz Leads the Way.

www.AeroClenz.com

AEROCLENZ AVIVE™ SYSTEM: IN-FLIGHT CONTINUOUS UV-C DISINFECTION

***Utilizing 265nm LEDs for optimal disinfection**, the AVIVE system creates a combination of continuous & targeted pathogen disinfection.*

CONTINUOUS-CLEAN ENGINE

CABIN

- Full-cabin illumination
- Cleans the air between passengers & crew
- Calculated emissions & advanced triple-tier sensors for continuous safe exposure

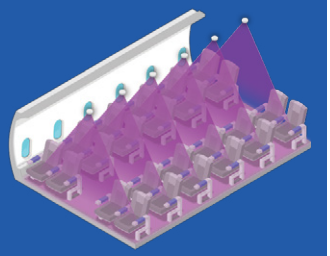

AISLE-SCRUB ENGINE

CABIN

- Targeted narrow beam
- Equivalent to 30 - 120 air exchanges per hour
- 90% airborne pathogen inactivation in < 3 minutes
- Intelligent sensors detect occupancy and control UV-C emission

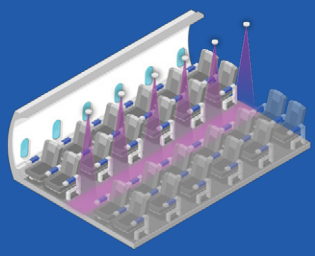

LAVATORY-SCRUB ENGINE

LAVATORY

- Full-lavatory coverage (air & surface)
- Equivalent to 600+ air exchanges per hour
- 90% inactivation: airborne pathogens in < 30 seconds, surface E. Coli in < 2 minutes
- Intelligent sensors detect occupancy & switch off when occupied

*Based on lab testing of actual airborne SARS-CoV-2, 90% of the virus is inactivated in less than 30 seconds.
*AeroClenz does not make any medical or health claims.
*Independent studies available upon request.

PROVEN TECHNOLOGY

AsMA Resolution

November 2023

The Aerospace Medical Association (AsMA) passed a resolution on the use of continuous inflight UV-C LEDs. The AsMA resolution specifically states: ***"The continuous use of UV-C aboard aircraft, below exposure limits, and with appropriate engineering safeguards, can be an additional synergistic, safe, and effective risk-mitigation layer to reduce disease transmission and translocation."***

UV-C Aircraft Disinfection Risk vs. Benefit Analysis

- "The **estimated annual economic burden** due to transmission of SARS-CoV-2 and Influenza A aboard U.S. commercial aircraft **was $200 billion.**"
- "**Up to 80% of the annual deaths and annual economic burden could be saved** by supplementing U.S. commercial aircraft with UV-C air disinfection."
- "**The one-time cost of implementing UV-C** disinfection on all U.S. commercial aircraft amounts to approximately 10% of the ongoing annual economic burden, or an estimated **1000% return on investment** every year after the one-time initial UV-C investment."

Boost Profits, Enhance Health!

Interested in UV-C Systems for Indoor Environments?

AeroClenz is proud to also offer the AdaptUV System™, the robust UV-C disinfection tailored for diverse indoor environments such as medical facilities, airports, gyms, government buildings, offices, and more. Learn more at: ***www.AeroClenz.com/Indoor-Solutions***

REAL-TIME DISINFECTION

LEADING PERFORMANCE

UV

CONTINUOUS SAFETY

DISINFECTION THAT **ADAPTS**

Risk vs. Benefit Analysis of Ultraviolet-C Advanced Aircraft Disinfection

Gary R. Allen; William D. Mills; Diego M. Garcia

INTRODUCTION: This work provides details and references that help to quantify the benefits of using ultraviolet-C (UV-C) light for air disinfection in aircraft vs. the risk of overexposure to UV-C for passengers and crew. The analysis estimates that due to the combined transmission of Severe Acute Respiratory Syndrome Coronavirus 2 and Influenza A aboard commercial aircraft in the United States over the 3 yr through May 2023, there were on the order of 10,000 annual deaths, declining to 3,000/yr going forward, with an estimated annual economic burden of $200 billion. Up to 80% of the deaths and economic burden might be saved by supplementing the typical 30 air changes per hour of the aircraft ventilation system with a presently available 120 air changes per hour, using a UV-C disinfection system. The risks due to accidental overexposure to UV-C are orders of magnitude lower than the benefits. The 0.00003% risk of acute (one-time) overexposure for any given passenger may (or may not) result in a 1–2-day skin or eye irritation, with no long-term effects or risks, compared to the 15,000 times greater risk, at 0.5%, of contracting coronavirus disease 19 or Influenza A that persists for several days to weeks, and carries a risk of hospitalization or death. The estimated risk of non-melanoma skin cancer is virtually nil.

KEYWORDS: ultraviolet, UV-C, disinfection, aircraft, ventilation, airborne, pathogen, severe acute respiratory syndrome coronavirus 2, SARS-CoV-2, coronavirus disease 19, COVID-19, influenza, transmission, risks, benefits, infections, deaths.

Allen GR, Mills WD, Garcia DM. *Risk vs. benefit analysis of ultraviolet-C advanced aircraft disinfection*. Aerosp Med Hum Perform. 2025; 96(3):A1–A32.

The purpose of this manuscript is to provide details and references that can help to quantify the benefits of using ultraviolet-C (UV-C) light for air disinfection in aircraft vs. the risk of overexposure to UV-C for passengers and crew with order-of-magnitude precision (i.e., within a range from approximately three times lower to three times higher than the calculated estimate). Some of the data inputs to the calculations are no more precise than approximately a factor of two. Improving the precision of calculations in future studies will require higher precision data along with sensitivity analyses.

Summary of Conclusions

1. There were an estimated 10,000 annual deaths due to transmission of Severe Acute Respiratory Syndrome Coronavirus 2 (SARS-CoV-2) and Influenza A, combined, aboard U.S. commercial aircraft for the 3-yr period ending May 2023. This rate has since declined to an estimated 3000/yr. The ongoing annual death toll from airborne disease transmission aboard U.S. commercial aircraft is on the order of 10–100 times greater than the annual death toll from U.S. commercial airline crashes prior to 1990. The authors rigorously cross-checked these results using two independent methodologies (shown herein), along with confirmation by an epidemiological statistics expert.
2. The estimated annual economic burden due to transmission of SARS-CoV-2 and Influenza A aboard U.S. commercial aircraft during the period February 2020 through September 2021 was $200 billion.
3. Up to 80% of the annual deaths and annual economic burden might be saved by supplementing the ventilation in all U.S. commercial aircraft with UV-C air disinfection.

From AeroClenz Inc., Fort Myers, FL, United States.

This manuscript was received for review in August 2023. It was accepted for publication in December 2024.

Address correspondence to: Dr. Gary R. Allen, 7805 S. Zante Ct., Aurora, CO 80016, United States; gra6000@gmail.com.

DOI: https://doi.org/10.3357/AMHP.6351.2025

4. The one-time cost of implementing UV-C air disinfection on all U.S. commercial aircraft amounts to approximately 10% of the ongoing annual economic burden, or an estimated 1000% return on investment every year after the one-time initial investment.
5. The one-time installation cost of implementing UV-C air disinfection on all U.S. commercial aircraft, amortized across the estimated 3000–10,000 annual deaths over the estimated 20-yr life of the UV-C system, results in an estimated $10,000 cost per life saved.
6. The estimated 0.00003% risk of acute (one-time) overexposure for any given passenger may (or may not) result in a 1–2-d skin or eye irritation, with no long-term effects or risks, compared to the estimated 15,000 times greater risk (0.5%) of contracting COVID-19 or Influenza A that persists for several days to weeks and carries a risk of hospitalization or death.
7. There seems to be virtually no scenario for any occupant aboard an aircraft equipped with a UV-C system designed below the regulated Exposure Limit to receive a chronic, occupational dose of UV-C sufficient to increase the risk of nonmelanoma skin cancer (NMSC). Furthermore, malignant melanoma is not of concern from UV-C irradiation at these levels.
8. In a very unlikely scenario that could result in chronic, occupational overexposure to flight attendants, the estimated risk of even one flight attendant in the United States contracting NMSC over a 20-yr period from UV-C overexposure aboard the aircraft is 0.016%. That 0.016% of an NMSC case is highly treatable, at a cost of approximately $900 per treatment, or less than $10 considering the 0.016% probability of the occurrence of NMSC, with virtually no probability of even one death.
9. The ratio of economic benefits of avoiding illnesses and deaths from infectious disease relative to the risk of economic burden, or the risks of adverse health outcomes, from having UV-C onboard is greater than 10 billion to one.

Introduction

The confusion around transmission of COVID-19 and other airborne diseases aboard aircraft can finally be clarified. One does not need to rely on previous unsubstantiated claims like the ones quoted below, even though they had been provided by trusted authorities in the United States.

> *It's Almost Impossible to Get COVID-19 on an Airplane, New Military Study Suggests*[42] *SCOTT AIR FORCE BASE, Ill. – U.S. Transportation Command (USTRANSCOM) released the results from its Commercial Aircraft Cabin Aerosol Dispersion Test showing the overall exposure risk from aerosolized pathogens, like coronavirus, is very low on the type of aircraft the command contracts to move Department of Defense personnel and their families.*[50]
>
> *Even with these prevention methods, a small number of travelers arrive at their destination testing positive for the virus. There has been little clear evidence to date if the infections were contracted while aboard flights.*[50]

There have been historical inaccuracies in estimating the risk of transmission of airborne pathogens aboard aircraft. Even as recently as the 2021 USTRANSCOM report,[50] data were rigorously measured but incorrectly interpreted, leading to incorrectly assuring the safety of air aboard commercial aircraft in response to well-founded public fear of COVID-19 transmission aboard commercial aircraft.

The TRANSCOM report acknowledged that: "a small number of travelers arrive at their destination testing positive for the virus." But the report deflected the hard evidence that was mentioned in the report with the disclaimer: "[t]here has been little clear evidence to date if the infections were contracted while aboard flights."[50]

There had been "little clear evidence" because contact tracing had not been widely conducted in the United States. Hence, the transmission route of airborne disease in the United States had been infrequently established. Nonetheless, the USTRANSCOM-authored reference article on which the above statements are based provides the following evidence to the contrary:

> *An ideal case study on an 18-hour Boeing 777 flight was completed in part thanks to the unique pre-testing, and quarantining required by New Zealand. During this flight, which included a stop for refueling (with the air system disabled) and in-flight meals, four in-flight transmission events occurred amongst 14 passengers located within three rows of an index case.*[50]

The case study cited above is strong evidence of airborne transmission of disease aboard an aircraft. The reliability of the data was enabled by the extraordinary controls in place in New Zealand during the COVID pandemic, including 100% pretesting and post-quarantining of all passengers, so that illness prior to and following the flight were reliably determined.

Instead of relying on simulated testing of aerosols aboard the aircraft, as in the USTRANSCOM report, the present document quantitatively and empirically estimates the occurrence of transmission of COVID-19 and Influenza A aboard aircraft using data extracted from a peer-reviewed systematic analysis[45] of all highly reliable epidemiological data displaying transmission of airborne diseases aboard aircraft. Most of these data were available prior to the USTRANSCOM report.

There is recently emerging, statistically significant analysis of onboard transmission of airborne diseases in the aircraft cabin[45] that now displaces the historical claims of lack of evidence that have been the mainstay response of the airline industry. Below is an excerpt from the abstract of the peer-reviewed 2023 Rafferty article:

> *Overall, 43.7% (72/165) of investigations provided evidence for in-flight transmission. H1N1 influenza A virus had the highest reported pooled attack rate per 100 persons (AR = 1.17), followed by SARS-CoV-2*

(AR = 0.54) and SARS-CoV (AR = 0.32), Mycobacterium tuberculosis (TB, AR = 0.25), and measles virus (AR = 0.09). There was high heterogeneity in estimates between studies, except for TB. Of the 72 investigations that provided evidence for in-flight transmission, 27 investigations were assessed as having a high level of evidence, 23 as medium, and 22 as low. One third of the investigations that reported on proximity of cases showed transmission occurring beyond the 2 × 2 seating area.[45]

It is clear that the well-intended, yet inconclusive, analyses of the past can now be superseded by the power of meta-analysis and standard analytical formalisms using statistically significant datasets in more recent studies of onboard transmission of infectious diseases. An example of a well-intended but non-committal report from the past, a 2002 National Research Council (NRC, the operating arm of the U.S. National Academies) study that was a follow-up to their 1986 study, included conclusions as excerpted here:

A person's risk of acquiring an infection on an aircraft depends on several factors, such as the presence of an infectious person and release of infectious agents by that person, the ventilation rate and mixing of cabin air, the amount of air that is recirculated and how it is treated, proximity to the source person, duration of exposure, and susceptibility to the specific infectious agents. These factors could also increase inhalation exposure to allergens and other potentially hazardous biological materials generated by passengers and activities within aircraft cabins.

The proper design, operation, and maintenance of an aircraft ventilation system can limit but not eliminate the transmission of infectious agents and exposure to other biological agents on aircraft. Exposure to biological agents is increased when people are confined in an aircraft cabin without adequate ventilation.[39]

The above conclusions from the 2002 NRC report regarding transmission of infectious diseases is not nearly as impactful as the 1986 recommendation regarding smoking that, in fact, resulted in banning smoking aboard U.S. commercial aircraft, as excerpted here from the 2002 NRC report:

That [1986] report recommended the elimination of smoking on most domestic airline flights and a number of other actions to address health and safety problems and to obtain better data on cabin air quality. In response to that report, the Federal Aviation Administration (FAA) took several actions, including the banning of smoking on all domestic flights.[39]

In fact, the 2002 report analyzed only two flights having statistically significant evidence of onboard transmission of Influenza A. The attack rates were extremely high: 38–72% on one flight and 12–53% on the second flight. Analyses of similarly limited numbers of flights were reported for measles, tuberculosis, and meningococcal disease.

One can now move beyond the limited and inconclusive studies of the past, such as the 1986 and 2002 NRC reports and the 2021 USTRANSCOM report,[50] neither of which made recommendations to reduce the risk of airborne disease transmission, and instead consider the more recent, powerful meta-analysis of the 2023 Rafferty[45] review publication. One can now quantify, rather than dismiss, the risk of transmission of infectious diseases onboard commercial aircraft.

Recommendation

Based on the estimates of illnesses, deaths, and economic burden presented in this document, supported by peer-reviewed datasets and analytical formalisms, it is recommended that the airline industry greatly improve the air quality aboard aircraft to reduce the risk of onboard transmission of infectious diseases in the same manner as they eliminated the health risks and burdens from smoking aboard aircraft.

EPIDEMIOLOGICAL METHODOLOGY

Estimating the Unmanaged Residual Risk Due to Seasonal Influenza

The excess burden from onboard transmission of influenza can be estimated in several ways, including excess illness, excess deaths, or estimated economic costs. This exercise examines the impact of onboard transmission of infection on U.S. commercial air carriers using epidemiological data for routine seasonal influenza for the 10 yr from 2010–2019 and the severe period of the COVID-19 pandemic from February 2020 through September 2021. The numbers are larger than one might expect due to the extremely high density of passengers per cabin volume, as described in the Wells-Riley mechanistic section of this work, below.

It was estimated that for a typical year, onboard transmission on U.S. commercial air carriers of seasonal influenza was responsible for infection of 473,800 passengers, who would have transmitted the infection to an additional 473,800 people in the general U.S. population for a total of 947,600 infections, counting only the first wave of secondary infections. This amounts to 3.2% of all seasonal influenza in the United States being due to transmission aboard commercial aircraft. Mortality resulting from onboard transmission of seasonal influenza infections is estimated herein at 38 deaths of passengers infected onboard, plus 599 deaths from the first wave of secondary infections for an estimated total of 637 deaths. This accounts for 1.7% of all U.S. deaths from seasonal influenza. Independent mechanistic Wells-Riley calculations included in this work produced similar results, further below.

The COVID-19 pandemic was devastating for the United States as well as the rest of the world. The February 2020 through September 2021 time period covers most of the U.S. Delta wave epidemic. For this 20-mo period, it is estimated herein that onboard transmission of COVID-19 on U.S. air carriers resulted in infection of 1,058,330 passengers, who

would have transmitted the infection to an additional 1,058,330 people in the general population for a total of 2,116,660 infections. Again, this counts only the first wave of secondary infections. Even this conservative estimate indicates that onboard transmission was responsible for 1.4% of all COVID-19 infections in the United States during this 20-mo period. Mortality resulting from onboard transmission of pandemic COVID-19 infections was estimated to be 2070 deaths of passengers infected onboard, plus 6650 deaths from the first wave of secondary infections for a total of 8720 deaths over this 20-mo period of the pandemic. This amounts to approximately 0.9% of all deaths from COVID-19 over this 20-mo period being due to onboard transmission. Note that these large numbers were in spite of the fact that the number of flying passengers was greatly reduced during this period and that masks were mandated starting around May 2020. The total societal cost for onboard transmissions of seasonal influenza is estimated to be $1.6 billion, or $1688 per illness. For a disaster like the COVID-19 pandemic, the cost of onboard transmission of COVID-19 could be $204 billion, or $96,567 per onboard transmission of COVID-19.

Estimating the Excess Number of Seasonal Influenza Infections Due to Onboard Transmission

The process flow for this calculation is as follows:

1. Project the U.S. Centers for Disease Control (CDC) seasonal influenza risk for each age group of the general U.S. population onto the age distribution of the flying population;
2. Multiply by the size of the flying population to yield the annual number who contract seasonal influenza;
3. Multiply by the risk that they will be flying on a day when they are contagious;
4. Multiply by the effective reproduction number for onboard transmission to estimate the number of onboard transmissions of seasonal influenza;
5. Obtain the number of these onboard transmissions that result in death the same way by projecting the CDC seasonal influenza mortality risk to the age distribution of airline passengers; and then
6. Calculate the number of infections and deaths in the general population due to these individuals who were infected onboard by applying a summary reproduction number for the general population to the group who were infected onboard airliners.

In this analysis the infectious passengers are considered as the source of infection, those infected onboard as primary infections, and succeeding infections transmitted postflight as secondary infections. For the calculation below, the averages for seasonal influenza over the 10-yr period from 2010–2019 will be used. The data used and the results of the calculations, per the process flow enumerated above, are provided in the following tables.

Data for the size of the U.S. population by year are displayed in **Table I**.[57] The risk of contracting influenza for each CDC age group by year is displayed in **Table II**.[16] The number of annual passengers on U.S. airlines can be obtained from the U.S. Bureau of Transportation Statistics[12] and is displayed in **Table III**. The proportion of the flying public in **Table IV** in each CDC age group was estimated by first locating passenger age groups for the United States (1984),[12] United Kingdom (1998),[41] and United Kingdom (2017),[20] and then extrapolating from the age groups in those data to the CDC age groups.

Table I. Annual U.S. Population 2010–2020.[57]

YEAR	ANNUAL U.S. POPULATION	MID-YEAR POPULATION
1/1/2010	309,327,143	310,455,312
1/1/2011	311,583,481	312,730,572
1/1/2012	313,877,662	314,968,805
1/1/2013	316,059,947	317,223,138
1/1/2014	318,386,329	319,562,662
1/1/2015	320,738,994	321,905,375
1/1/2016	323,071,755	324,096,942
1/1/2017	325,122,128	325,980,164
1/1/2018	326,838,199	327,584,076
1/1/2019	328,329,953	329,915,517
1/1/2020	331,501,080	---
Average from 2010–2019		320,442,256

The annual number of passengers in each CDC age group can be calculated in **Table V** as (average annual passengers × proportion in each age group). Then the number in each group estimated to have contracted influenza during the year can be calculated by: (annual passengers in each group × incidence in that group.) This is displayed in **Table VI**. So, the estimated annual proportion of airline passengers with influenza = (total passengers with influenza)/(total passengers) = 69,000,000/798,000,000 = 0.09. This is approximately the same as the average annual proportion of the total U.S. population with influenza for 2010–2019, which is approximately 8%.[17]

Now the daily number of airline passengers who are contagious with influenza can be calculated. The number of days influenza is contagious is addressed by the CDC.[17] A reasonable number for the duration that influenza is contagious is 5 d. The proportion of a year = (duration)/365.25 = 0.014. One can estimate that the proportion of these passengers who will fly even though they have symptoms is approximately 0.5. Influenza can certainly make one feel bad, but many passengers will endure that to get back home or to their destination. So, the chance that an individual will be infectious on a day they are flying = (duration/365.25) × (% flying with symptoms, S_x) = 0.014 × 0.5 = 0.007. The daily number of infectious passengers = (duration/365.25) × (% who fly with S_x) × (# annual passengers with influenza) = 0.07 × 69 million = 473,814.

Calculating the number of onboard transmissions requires knowing the overall effective reproduction number (R_e) for influenza averaged over the flu season. It is known that R_e must be >1 in the first part of the season and <1 toward the end of the season. Note that the epidemic curve for an average flu season

Table II. Estimated Rates of Symptomatic Influenza, Per 100,000, by Age Group.[16]

YEAR	0–4 yr	5–17 yr	18–49 yr	50–64 yr	65+ yr
2010 to 2011	13,743	8217	5468	8241	4521
2011 to 2012	4697	3712	2564	3181	2334
2012 to 2013	17,821	12,419	8384	12,852	9712
2013 to 2014	12,712	7416	9590	13,713	3819
2014 to 2015	16,136	11,895	6310	11,626	10,120
2015 to 2016	11,028	7705	6668	10,505	2946
2016 to 2017	11,950	12,012	6786	11,766	7404
2017 to 2018	17,086	13,332	9931	18,385	10,096
2018 to 2019	15,239	12,359	7088	11,439	4287
2019 to 2020	19,519	13,404	10,432	13,747	13,747
Average	14,021	10,472	7528	11,913	7163
Median	15,239	12,012	7088	11,766	7404
Med Fraction	0.15	0.12	0.07	0.12	0.07

is fairly symmetric.[18] The case studies for onboard transmission of influenza in the Rafferty article[45] show a pooled secondary attack rate of 0.0117 and a crude reproductive number of 2.28. So, with an average of approximately 100 passengers per flight, it seems reasonable to assume the R_e for onboard transmission over the season is approximately 1.0. Note that the average R for seasonal influenza in the general population is usually approximately 1.3.[8,37] So, the total number of annual onboard transmissions of influenza = $R_e \times$ (# infectious) = 473,814.

As above, assume the seasonal R_e for the general U.S. population is also approximately 1. Assume random postflight mixing of passengers infected onboard with the general U.S. population. So, the total number of secondary cases due to the onboard infected = (the number infected onboard) $\times$ R_e = 473,814 × 1 = 473,814. Then the estimated total annual number of influenza cases caused by onboard transmission is: (# infected onboard) + (# secondary infections from that group) = 473,814 + 473,814 = 947,629. This includes only the first wave of secondary infections for simplicity, but there would be additional waves of infection related to the group infected onboard. The above estimate indicates that onboard transmission of influenza is responsible for 3.2% of all seasonal influenza in the United States.

Table III. Annual Number of Passengers on U.S. Airlines in Millions.[12]

YEAR	NO. OF PASSENGERS
2010	720
2011	731
2012	737
2013	743
2014	763
2015	798
2016	824
2017	849
2018	889
2019	926
Average	798

Table IV. The Proportion of Passengers in Each CDC Age Group.[20,41,43]

AGE GROUP (yr)	2017 UK	1984 U.S.	1998 UK	AVERAGE
0–4	0.01	0.03	0.02	0.02
5–17	0.05	0.08	0.08	0.07
18–49	0.59	0.63	0.61	0.61
50–64	0.25	0.18	0.23	0.22
65+	0.10	0.09	0.07	0.09

Estimating the Excess Influenza Mortality Due to Onboard Transmission

The CDC published the general population mortality burden for 2010–2019 and analogous pages for earlier years.[16,37] The median number of deaths from influenza in the United States from 2010–2019 is 37,293. The annual median number of symptomatic influenza cases over this same period is 29,480,259. So, the number of deaths in the general population related to secondary infection from the onboard infected passengers = (U.S. deaths/U.S. cases) × (cases transmitted onboard) = (37,293/29,480,259) × 473,814 = 599. There would be additional deaths from tertiary infections from this group, but these are also omitted for simplicity and to be conservative.

A number of the passengers infected onboard will also die. Calculating this more accurately requires accounting for the

Table V. Annual Number of Passengers in Millions for Each CDC Age Group.

AGE GROUP (yr)	MILLIONS OF PASSENGERS
0–4	15.43
5–17	54.64
18–49	487.13
50–64	175.37
65+	69.51

Table VI. Annual Number of Passengers in Millions in Each Age Group Expected to Have Influenza.

AGE GROUP (yr)	PASSENGERS WITH INFLUENZA
0–4	2.35
5–17	6.56
18–49	34.53
50–64	20.63
65+	5.15
Total	69.22

Table VII. Estimated Mortality Rates for Influenza, Per 100,000, by Age Group.[16]

YEAR	0–4 yr	5–17 yr	18–49 yr	50–64 yr	65+ yr
2010–2011	1	0.3	3.9	10.1	62.4
2011–2012	0	0	0.5	3.8	22.6
2012–2013	1.5	1.6	1.5	6.8	81.5
2013–2014	0.4	0.1	2.5	9.6	63.6
2014–2015	2	0.8	0.7	7.6	96.9
2015–2016	0.9	0.2	1.2	5.2	36.6
2016–2017	0.6	0.2	1	6	66.7
2017–2018	0.5	0.8	1.6	9.2	84.6
2018–2019	1.1	0.3	1.2	7	40.5
2019–2020	1.7	0.3	1.9	9.8	29.4
Average	1.0	0.5	1.6	7.5	58
Median	1.0	0.3	1.4	7.3	63

age distribution of the flying public since the mortality rate varies between age groups and age distribution of the flying public is different. The median mortality rate from 2010–2019 from influenza for the CDC age groups is displayed in **Table VII**.[16] To obtain the mortality rate per 100,000 for the onboard infected passengers: SUM OVER [(proportion of passengers in each age group) × (median mortality rate/100,000 for the age group)]. The proportion of the flying population in each age group is displayed in **Table VIII**. This results in a mortality rate per 100,000 onboard infected passengers equal to 8.

The total number of deaths in this group = (# onboard infected passengers) × (mortality rate per 100,000)/100,000 = 473,814 × 8/100,000 = 38. Note that this number is a fraction of the 599 general population deaths due to the much smaller proportion of 65+-year-olds in the flying population and the high mortality in the 65+-year-old group in the general population. The estimated total median number of annual deaths related to onboard transmission of influenza from 2010–2019 = (deaths of onboard infected passengers) + (deaths in general population who were infected from the infected passengers) = 38 + 599 = 637. Overall, it is estimated that the annual impact of onboard transmission of influenza for the period 2010–2019 amounts to 947,629 infections and 637 deaths. So onboard transmission is estimated to be responsible for 3.2% of symptomatic influenza cases in the United States and 1.7% of all deaths from influenza.

Table VIII. Passengers in Each Age Group.

AGE GROUP (yr)	MILLIONS OF PASSENGERS
5–17	57.77
18–49	515.07
50–64	185.44
65+	73.49

Estimating the Excess Number of COVID-19 Infections Due to Onboard Transmission During the Period February 2020 through September 2021

The process flow for this calculation is similar to the estimate above for onboard infections of seasonal influenza. It requires projecting the CDC COVID-19 risk for each age group of the general U.S. population onto the age distribution of the flying population. Then multiplication by the size of the flying population yields the annual number who contract COVID-19. That is multiplied by the risk that they will be flying on a day when they are contagious. Then multiplication by the effective reproduction number for onboard transmission will estimate the number of onboard transmissions of COVID-19. The number of these onboard transmissions that result in death is accomplished the same way by projecting the CDC COVID-19 mortality risk to the age distribution of airline passengers. The number of infections and deaths in the general population due to these individuals who were infected onboard is calculated by applying a summary reproduction number for the general population in the group who were infected onboard airliners. In this analysis, the infectious passengers are considered as the source of infection, those infected onboard as primary infections, and succeeding infections in the general population as secondary infections.

The midpoint U.S. population during the February 2020 through September 2021 time period was 331,697,413.[57] The age-specific rates per 100,000 for COVID-19 are shown in **Table IX**.[16] The number of passengers on U.S. airlines, in millions, was 369 in 2020 and 674 in 2021.[12] From February 2020 through September 2021, there were an extrapolated 844 million passengers. From Table VIII, the proportion of passengers in these CDC age groups are: 5–17 yr (0.07), 18–49 yr (0.61), 50–64 yr (0.22), and 65+ yr (0.09). The total number of passengers in millions for each age group from February 2020 through September 2021 is (total passengers) × (proportion in each age group), as displayed in Table VIII.

Table IX. Age-Specific Rates of COVID-19 Infection Per 100,000 from February 2020 Through September 2021.[16]

PARAMETER	0–17 yr	18–49 yr	50–64 yr	65+ yr	ALL AGES
Infection Rate	35,490	54,860	43,656	32,363	44,650
Proportion	0.35	0.55	0.44	0.32	0.45

Table X. Passengers in Each Age Group Expected to Have COVID-19.

AGE GROUP (yr)	MILLIONS WTH COVID-19
5–17	20.50
18–49	282.57
50–64	80.95
65+	23.78

The number of passengers in each age group estimated to have COVID-19 from February 2020 through September 2021 is (the passengers in each group) × (incidence in that group), as displayed in **Table X**. So, the total number of passengers, in millions, estimated to have COVID-19 from February 2020 through September 2021 is 407.81.

The proportion of these airline passengers with COVID-19 is 0.48 (407.81/844, from above) compared to 0.45 (see Table IX) for the U.S. population. The chance of any of these passengers flying on a day when they are contagious depends on their duration of infectivity and the proportion who will fly when they may not be feeling well. The duration of infectivity for COVID-19 is approximately 5 d.[14] The proportion of this 20-mo period would be: (duration)/578 = 5/578 = 0.009. A modeling study estimated that 59% of the COVID-19 infections are from asymptomatic transmission,[30] so assume that 60% of passengers will fly when they are infectious. The probability that any given passenger on any given flight will be infectious on a day they are flying = (duration/578) × (% flying with symptoms) = (5/578) × 60% = 0.00519. So, the estimated number of infectious passengers flying = (proportion flying infectious) × (passengers with COVID during the 20 mo) = 0.00519 × 407,810,000 = 2,116,668.

The Rafferty systematic review[45] reports that the onboard secondary attack rate for COVID-19 was 0.54%, which, assuming 100 passengers per aircraft, translates roughly into an R_e of 0.5. Note that mask use was mandatory for most of this time period. So, the number of COVID-19 infections transmitted onboard = R_e × (# contagious) = 0.5 × 2,116,668 = 1,058,334.

This group will result in additional infections as they mix with the general U.S. population. The number of direct secondary infection is 1,058,334 × R_e. Choosing a summary R_e for these 20 mo is challenging. However, it is known that as the pandemic is expanding, R_e is greater than one, and when it is contracting, R_e is less than 1. Many expect that COVID will become endemic in the United States and, in this case, R_e would be approximately 1. The epidemic curve over these 20 mo covers most of the Delta wave and is relatively symmetric,[35,40] so an overall R_e = 1 was chosen. Note that this 20-mo period ends just before the much larger Omicron wave, which would have produced higher counts of onboard transmission. So, the number of secondary infections in this first wave equals 1,058,334.

Combined with the number of COVID-19 infections transmitted onboard, the total number of infections due to onboard transmissions, including secondary infections, equals 2,116,668. The number infected from February 2020 through September 2021 in the U.S. population was 146,585,169, so the percent of all U.S. COVID-19 infections from onboard transmission = 2,116,668/146,585,169 = 1.4%. The annualized total number of infections = (total over 20 mo) × (12/20) = 2,116,668 × 0.6 = 1,270,001.

Estimating the Excess Number of COVID-19 Deaths Due to Onboard Transmission from February 2020 Through September 2021

The estimated burden of COVID-19 mortality in the general population of the United States from February 2020 through September 2021 was 921,371 deaths. The overall number of cases was 146,585,169 for a case fatality proportion of 0.00629.[15] So, the number of deaths in the general population over this 20-mo period due to secondary infection from the onboard infected passengers = (U.S. deaths/U.S. cases) × (secondary cases) = 0.00629 × 1,058,334 = 6652.

A number of the passengers infected onboard will also die. As for influenza, calculating this for COVID-19 requires accounting for the age distribution of the flying public since the mortality rate varies between age groups and age distribution of the flying public is different. The median mortality rates from COVID-19 for the CDC age groups are displayed in **Table XI**.[15] To obtain the mortality rate per 100,000 for the onboard infected passengers, SUM OVER [(proportion of passengers in each age group) × (median mortality rate/100,000 for the age group)]. The proportion of the flying population in each age group is displayed in Table VIII. This results in the median mortality rate per 100,000 infected onboard passengers for each age group as follows: 0.06 for 0–17 yr, 26.68 for 18–49 yr, 55.71 for 50–64 yr, and 112.93 for 65+ yr.

So (total passenger deaths)/(100,000 infected onboard passengers) = 195.37. The total deaths of the onboard infected passengers then equals: (deaths per 100,000 infected onboard passengers) × (# onboard infected passengers)/100,000 = 195.37 × 1,058,334/100,000 = 2068. Note that this number is a fraction of the general population deaths (6652) due to the much smaller proportion of 65+-year-olds in the flying population and the high mortality in the 65+-year-old group in the general population. The estimate for total deaths attributed to onboard transmission of COVID-19, including secondary deaths in the general population, is 8720. The annualized total number of deaths = (total over 20 mo) × (12/20) = 8720 × 0.6 = 5232. The total number of COVID deaths in the general population over 20 mo = 921,371. So, the percentage of COVID-19 deaths due to onboard transmission is 0.9%. Note

Table XI. Mortality Rates for COVID-19, Per 100,000, by Age Group.[15]

YEAR	0–17 yr	18–49 yr	50–64 yr	65+ yr	ALL AGES
2020–2021	0.9	43.7	253.5	1296.5	280.7
Proportion	0.0000	0.0004	0.0025	0.0130	0.0028

that this counts only the secondary infections from the onboard infected passengers. There would be additional waves of infection from this group that, to be conservative, are not counted here. Also note that this large number was in spite of the fact that the number of flying passengers was greatly reduced during this period and that masks were mandated starting around May 2020.

Estimating the Economic Impact of Onboard Transmission of Seasonal Influenza

There are a number of studies exploring the economic cost of seasonal influenza. A 2007 publication appears to be the most cited, likely because it answers the question most clearly.[37] Other newer studies are less helpful because they focus on subsegments of the population.[22,48] The Molinari[37] paper reports $10.4 billion ($4.1–$22.2 billion, 95% confidence interval) in direct medical costs with a total economic burden of $87.1billion ($47.2–$149.5 billion). A 2018 paper by Putri[44] estimated direct medical costs at $3.2 billion ($1.5–$11.7 billion) and lost work time at $8.0 billion ($4.8–$13.6 billion) for a total economic cost of $11.2 billion ($6.3–$25.3 billion). All of his measures are smaller than the actual CDC reports. Most notably he estimated 4.4 million outpatient visits compared to median CDC-reported 13.5 million annual visits for the 2010–2019 timeframe. Molinari[37] overestimated medical visits at 31.4 million and included projected statistical life values in the overall societal cost. An estimate of all societal costs would include direct medical costs of $10 billion with a total societal cost of $50 billion. The interested reader can substitute other estimates in the calculations below, but the results should be approximately the same. From above, the percentage of all influenza cases resulting from onboard transmission is 3.2%. So, the estimate of direct medical cost from onboard transmission is $320,000,000, and total societal cost from onboard transmission is $1.6 billion. The total cost per each onboard transmission of flu is estimated at $1688.

Estimating the Economic Impact of Onboard Transmission of Pandemic COVID-19

Estimation of the economic impact on the United States from the COVID-19 pandemic is difficult because of its enormous scale. One article suggests an economic impact of $16 trillion in the United States.[21] This includes the economic cost of premature deaths at $4.4 trillion, economic cost of long-term complications at $2.6 trillion, mental health impairment in the general population at $1.6 trillion, and lost productivity at $7.6 trillion. The total estimated U.S. economic burden, excluding the mental health category, is $14.6 trillion. So, the 1.4% of COVID-19 infections due to onboard transmission accounts for approximately $204 billion or approximately $96,567 per onboard transmission of COVID-19. For direct medical expenses alone, the cost per symptomatic patient has been modeled at $3037–3994.[6,46] For the February 2020 through September 2021 time period the CDC estimated 123,979,337 (111,032,406–139,954,539) cases of symptomatic COVID-19.[15] Assuming $3500 per symptomatic patient yields an estimated direct medical cost of $6.1 billion in the United States.

WELLS-RILEY FORMALISM TO ESTIMATE RESIDUAL RISK OF INFECTION OR DEATH NOT EFFECTIVELY MITIGATED BY VENTILATION AND MASKS ABOARD AIRCRAFT

A typical approach in quantifying the risk of airborne transmission of disease in an indoor environment is presented in two independent research papers.[11,43] A thorough description of the Wells-Riley formalism as applied to airborne transmission of SARS-COV-2 is provided in Peng,[43] starting with the rate equation for the (assumed uniform) concentration of pathogen quanta in the space (a quantum is defined as the dose of airborne droplet nuclei required to cause infection in 63% of susceptible persons):

$$\frac{dc}{dt} = \frac{E_p \times f_e}{V} - \left(\lambda_0 + \lambda_{dec} + \lambda_{dep} + \lambda_{cle}\right) \times c \qquad \text{Eq. 1}$$

Where: E_p is the emission rate of quanta into the indoor air from an infected person in the space (quanta/h); f_e is the penetration efficiency of virus-carrying particles through masks or face coverings for exhalation; V is the volume of the space (m^3); λ_0 is the removal rate (/h) of quanta by ventilation with outdoor or filtered air, e.g., HVAC; λ_{cle} is the removal rate (/h) of quanta by air cleaning devices; (e.g., recirculated air with filtering, germicidal UV, portable air cleaners, etc.); λ_{dec} is the natural infectivity decay rate (/h) of the virus; and λ_{dep} is the deposition rate (/h) of airborne virus-containing particles onto surfaces.

In the regimes of interest for air disinfection inside aircraft cabins, the rates λ_0 (outdoor air) and λ_{cle} (due to germicidal UV) dominate all the other removal rates, since λ_{dec} and λ_{dep} are less than 1/h.[43] Further, without mask wearing, $f_e = 1$, so that Eq. 1 simplifies to:

$$\frac{dc}{dt} = \frac{E_p}{V} - \left(\lambda_o + \lambda_{cle}\right) \times c \qquad \text{Eq. 2}$$

DISINFECTION EFFICACY IN AIR FOR VENTILATION IN TERMS OF ACH

The removal rates, λ_0 and λ_{cle}, are more typically referred to in the air disinfection literature as air exchange rates (AER) quantified in air changes per hour (ACH), which is one of the standard metrics used to quantify air disinfection rates. The AER describes the total volume of air that flows through a room per hour divided by the room volume:

$$AER(\text{ACH}) = \frac{Q\left(\frac{m^3}{h}\right)}{V(m^3)}$$

Where: Q ($m^3 \cdot h^{-1}$) is the volume (m^3) of air that flows through a room per hour; and V is the volume (m^3) of the room.[56]

For example, if the volume, V, of an aircraft cabin is 100 m^3, and the total rate of air flow, Q, through the cabin by the ventilation system is 1000 $m^3 \cdot h^{-1}$, then the AER is 10 ACH. Traditional air cleaning technology used in aircraft includes the

introduction of outside air, and the filtering of recirculated air by the cabin ventilation system. Both the fresh outside air and the recirculated filtered air contribute to the ventilation rate in the aircraft cabin, ACH_{vent}. In the formalism of Eq. 1 and 2, the parameters λ_0 and λ_{cle} are equivalent to ACH_{vent} and ACH_{UV}, respectively.

The infection risk reduction due to the effects of ACH_{vent} and ACH_{UV} are most easily recognized when considering the steady-state situation which would obtain inside an aircraft cabin after all of the emission and removal rates equilibrated (emission rate of quanta by an infected passenger as well as removal of quanta by ventilation and UV). In steady state, the left side of Eq. 2 equals zero and substituting the parameters λ_0 and λ_{cle} with ACH_{vent} and ACH_{UV}, respectively, the steady-state concentration is given by:

$$c_{ss} = \frac{E_p}{V \times \left(ACH_{vent} + ACH_{UV}\right)} \qquad \text{Eq. 3}$$

In the baseline case with aircraft ventilation, but no UV disinfection, the steady-state pathogen concentration in the absence of UV disinfection reduces to:

$$c_{ss,vent} = \frac{E_p}{V \times ACH_{vent}} \qquad \text{Eq. 4}$$

Then, when UV disinfection is added (as in Eq. 3) to the aircraft ventilation (in Eq. 4), the steady-state concentration of airborne pathogens is reduced by a factor, R, obtained by taking the ratio of the two steady-state pathogen concentrations, as below in Eq. 5:

$$R \equiv \frac{c_{ss}}{c_{ss,vent}} = \frac{\left(\frac{E_p}{V \times \left(ACH_{vent} + ACH_{UV}\right)}\right)}{\left(\frac{E_p}{V \times ACH_{vent}}\right)} = \frac{ACH_{vent}}{ACH_{vent} + ACH_{UV}} \qquad \text{Eq. 5}$$

Exemplary results of Eq. 5 are presented in **Table XII**. The ACH_{vent} values of 15 and 30 represent a typical range for U.S. commercial aircraft while cruising, and 5 represents an approximate ACH_{vent} while on the ground. The ACH_{UV} values used herein (ranging from 30/h to 120/h) are attainable with present technology, depending on the wavelength of UV and the spacing of the UV emitters throughout the aircraft cabin.

Table XII indicates that the reduction of residual airborne pathogen concentration left over following removal by the aircraft ventilation system may be further reduced by the UV-C disinfection system by anywhere from 33–89% while cruising, and by up to 96% while grounded. A conservative value of R while cruising might equal 0.33 (a 67% reduction in airborne pathogen concentration by addition of UV-C to ventilation), corresponding to an ACH_{vent} equal to 30 and ACH_{UV} equal to 60. Present technology makes possible an ACH_{UV} of 120 whereby R = 0.20 (an 80% reduction in airborne pathogen concentration). The relative risk of infection will be shown later to be approximately proportional to R, i.e., the risk of infection by airborne diseases is estimated to be reduced by up to 80% by the addition of UV-C as supplemental infection mitigation on top of the onboard cabin ventilation system.

Table XII. R, the Ratio of the Steady State Concentration of Airborne Pathogens With vs. Without UV-C Disinfection.

	ACH_{UV}			
ACH_{vent}	**15**	**30**	**60**	**120**
5	0.25	0.14	0.08	0.04
15	0.50	0.33	0.20	0.11
30	0.67	0.50	0.33	0.20

ACH_{vent}: air changes per hour, ventilation rate; ACH_{UV}: air changes per hour, ultra-violet.

Above, the reduction of pathogen concentration accrued with UV-C has been estimated at R in the range of 0.20–0.33 (67–80% reduction in airborne pathogen concentration). One can evaluate the dose of quanta received by an exposed susceptible (not infected and not immune) individual and estimate the probability of infection on the basis of a dose–response model. The dose-response model generally used throughout the literature of airborne infection modeling is the Wells-Riley model,[43,45,47] whereby the probability that any susceptible individual will be infected, P_{indiv}, is given by:

$$P_{indiv} = 1 - e^{-n} \qquad \text{Eq. 6}$$

where n is the infectious dose (i.e., quantity of pathogens) inhaled by a susceptible person in the space, expressed in units of quanta. Accordingly, the risk of secondary infections increases linearly with n at lower values and nonlinearly at higher values, approaching 100% probability at extremely high concentrations, as demonstrated in **Fig. 1**. To interpret Fig. 1, when the inhaled quanta, n, equals zero, the risk of infection, P_{indiv}, is zero. For a "subcritical" inhaled dose of n equal to 0.1, the risk of infection is linearly proportional to n, so that $P_{indiv} \cong 10\%$. The term "quanta" is defined to be equal to one for that quantity of pathogens that, when inhaled by a susceptible individual, results in a risk of infection of $P_{indiv} \cong 63\%$. In the range of n on the order of one, the risk of infection vs. n becomes nonlinear, beginning to bend over toward the maximum possible 100%. As n increases beyond one, the risk of infection increases more nonlinearly, so that for n equal to two, $P_{indiv} \cong 86\%$, and for n equal to three, $P_{indiv} \cong 95\%$. For n much greater than three, P_{indiv} approaches the saturation value of 100%.

Note that many of the calculations and estimates in this work are limited in precision by the quality of the available data. The appropriate descriptor in such cases is "approximate" or "approximately," which may be interpreted to mean that the error bars, or range of validity, are from a few percentage points up to a factor of two or three. In contrast, some calculations and estimates in this work are uncertain within a factor of 3–10 or more. The appropriate descriptor in such cases is "on the order of" which means that the range of validity is an order of magnitude (a factor of 10) or greater.

An important insight from Fig. 1 is that when n is extremely low, e.g., n on the order of 0.001, and the risk of infection is

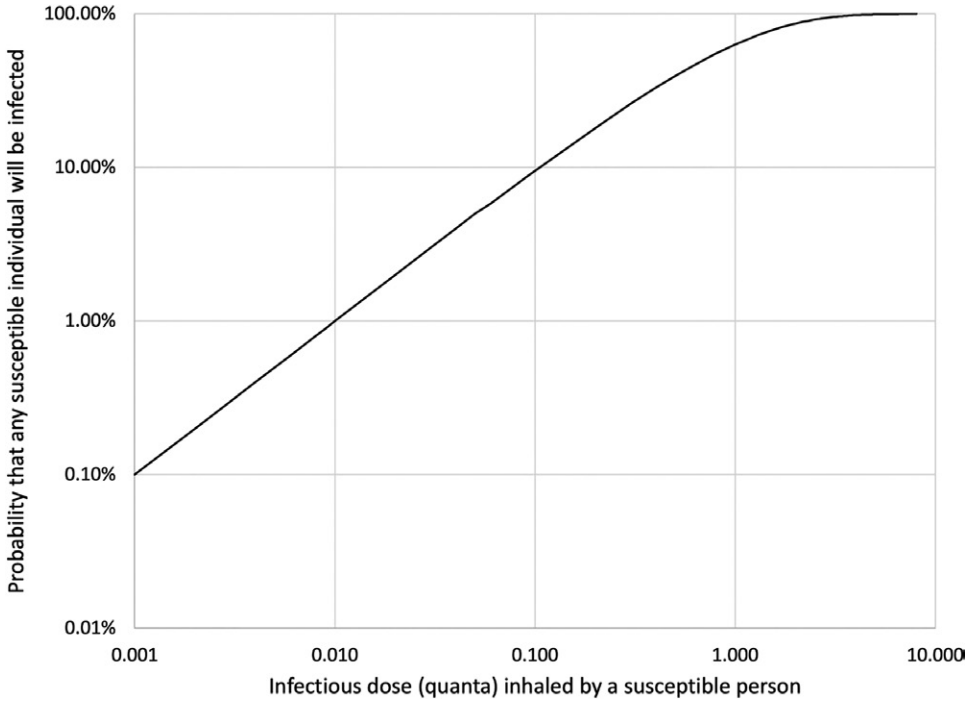

Fig. 1. The probability that any susceptible (not infected and not immune) individual will be infected, from Eq. 6.

extremely low, e.g., P_{indiv} is on the order of 0.1%, then taking auxiliary measures to further reduce the risk, such as using UV to further reduce n, provides a diminishing return and is not worth the cost. At the other extreme, when the pathogen concentration is so high, e.g., n greater than 10, so that $P_{indiv} \cong 100\%$, then taking auxiliary measures such as using UV to reduce n to five or more will reduce P by only a fraction of 1%, again providing diminishing returns.

To express this insight in intuitive terms, if n and P_{indiv} are extremely low, then we would have no evidence of passengers getting sick on airplanes—this is not the case. At the other extreme, if n is much greater than one and P_{indiv} is approximately 100%, then virtually everyone gets sick on every flight, and it is obvious that the risk must be severely reduced—this is also not the case. So, intuitively, the risk of infection aboard aircraft is significant and reducing n by the order of 2–10 times might be expected to significantly reduce the risk of infection and the resulting deaths and economic burdens. In the regime where some, but not most, of the susceptible individuals in the occupied space become infected, then the linear approximation of Eq. 6 is valid, as below.

In the linear (low risk) regime, where n is much less than one, a Taylor Series expansion simplifies Eq. 6 to:

$$P_{indiv} \cong n \qquad \text{Eq. 7}$$

For example, if n (the infectious dose inhaled by a susceptible individual) is 10% (0.10), then Eq. 6 results in a probability of infection, P_{indiv} = 0.0951…, whereas the approximation in Eq. 7 results in a P_{indiv} = 0.100, a 5% error, which can be neglected going forward given the objective of obtaining order of magnitude estimates. Note that the numerical results presented below in this work do not make the assumption of a linear regime, as in Eq. 7, but rather use the exact form of Eq. 6. The simplification obtained in Eq. 7 is used herein only to simplify the insights available from deriving the mechanistic infection risk methodology in closed analytic form that is enabled by the simplicity of Eq. 7. The probability, P_{indiv} = n, that any susceptible individual will be infected, given that one of the passengers is infectious, is quantified by Peng[43] by defining the three parameters appearing in the following equation:

$$P_{indiv} = 1 - e^{-n} \cong n = E_{p0} \times B_o \times H_r \qquad \text{Eq. 8}$$

where E_{p0} is the quanta shedding rate [the rate at which an infectious person exhales infectious doses, in quanta/hour, baselined to an infectious person at rest and only orally breathing (no vocalization)], and where B_0 is the average volumetric breathing rate ($m^3 \cdot h^{-1}$) of a sedentary susceptible person. E_{p0} is the minimum quanta shedding rate of an infectious individual before any enhancements of the shedding rate due to speaking, singing, physical activity, etc. B_0 is similarly the average volumetric breathing rate of a sedentary susceptible person before any enhancements due to physical activity. The fixed parameters, E_{p0} and B_0, are intrinsic to all infectious and susceptible individuals, while the factor H_r contains all the variable parameters in any specific situation, e.g., in the aircraft cabin as opposed to a terrestrial setting, and including enhancements due to speaking, singing, physical activity, etc.

Eq. 8 was derived for the probability that any susceptible individual will be infected assuming that one passenger was infectious. Then the probability, $P_{PAX,inf}$, that any susceptible

passenger, among all of the passengers onboard, will become infected, considering the probability, $P_{PAX,ill}$, that an infectious passenger is aboard a given flight, is given by:

$$P_{PAX,inf} = P_{PAX,ill} \times P_{indiv} = P_{PAX,ill} \times E_{p0} \times B_o \times H_r \quad \text{Eq. 9}$$

For use in Eq. 9, the probability that an infectious passenger is aboard a given flight is:

$$P_{PAX,ill} = N_{PAX} \times \%_{PAX,ill} \quad \text{Eq. 10}$$

In Eq. 10 above, the factor $\%_{PAX,ill}$ represents the percentage of passengers who are infectious on the day of the flight and who actually choose to fly while infected. This factor, $\%_{PAX,ill}$, is that fraction of the total U.S. population (pop) who are infectious and are ticketed for the flight that day, who actually choose to fly, in spite of their infection, denoted by $\%_{fly}$ in Eq. 11 below:

$$\%_{PAX,ill} = \%_{pop,ill,day} \times \%_{fly} \quad \text{Eq. 11}$$

Combining Eq. 9–11 above provides the probability, $P_{PAX,inf}$, that any individual susceptible passenger will become infected, considering the probability, $P_{PAX,ill}$, that an infectious passenger is aboard a given flight, given by:

$$P_{PAX,inf} = N_{PAX} \times \%_{pop,ill,day} \times \%_{fly} \times E_{p0} \times B_o \times H_r \quad \text{Eq. 12}$$

The estimated total number of passengers (PAX) who will be infected on any given flight, $PAX_{flight,inf}$, is then the probability, $P_{PAX,inf}$, that any susceptible passenger will become infected, from Eq. 12, times the number of passengers on the flight, N_{PAX}:

$$PAX_{flight,inf} = P_{PAX,inf} \times N_{PAX} = N_{PAX} \times N_{PAX} \times \%_{pop,ill,day} \times \%_{fly} \times E_{p0} \times B_o \times H_r \quad \text{Eq. 13}$$

The variable parameters in any specific situation in Eq. 13 are bundled into the "relative risk factor," H_r, which has units of $h^2 \cdot m^{-3}$ where:

$$H_r \equiv \frac{r_{ss} \times r_E \times r_B \times f_e \times f_i \times D}{V \times ACH_{tot}} \quad \text{Eq. 14}$$

The variable parameters in H_r in Eq. 14 include: r_{ss} equals one in steady-state equilibrium; r_E, the shedding rate enhancement factor relative to E_{p0} corresponding to the activity of an infectious individual displaying a certain degree of vocalization and physical intensity; r_B, the relative breathing rate enhancement factor (relative to B_0) for the activity of a susceptible person with a certain physical intensity and for a certain age group; f_e and f_i, the penetration efficiency of virus-carrying particles through masks or face coverings for exhalation and inhalation, respectively; D, the duration of the exposure (h); V, the volume of the space (m^3); and ACH_{tot}, the total removal rate of airborne pathogens including ACH_{vent} and ACH_{UV}.

Substituting Eq. 14 for H_r into Eq. 13 provides all the necessary inputs to calculate the estimated total number of passengers who will be infected on any given flight, $PAX_{flight,inf}$:

$$PAX_{flight,inf} = N_{PAX}{}^2 \times \%_{pop,ill,day} \times \%_{fly} \times E_{p0} \times B_o \times \frac{r_{ss} \times r_E \times r_B \times f_e \times f_i \times D}{V \times ACH_{tot}} \quad \text{Eq. 15}$$

In Eq. 15, the shedding and breathing rate enhancement factors, r_B and r_E, quantify the higher rates of shedding and inhalation for infected and susceptible individuals based on their level of vocalization and physical activity, which are excerpted in **Table XIII** and **Table XIV**, respectively, from Peng,[43] and the references therein. The intrinsic factors, E_{p0} and B_0, are the baseline rates of shedding virus and inhaling virus, for infected and susceptible individuals, respectively, who are sedentary and not vocalizing (talking, singing, coughing, sneezing, etc.), as follows:

E_{p0} is the quanta shedding rate of an infectious person resting and only orally breathing (no vocalization), which accounts for the amount of virus shed, the infectivity of each virus shed, and the susceptibility of the person who became infected, for a particular airborne pathogen;

B_0 is the average volumetric breathing rate (m^3/h) of a sedentary susceptible person (under the assumption of the same size of all age groups). It is estimated in the literature to be approximately 0.288 m^3/h.[43]

Considering the typical activities of passengers and crew aboard an aircraft, physical activity might range from resting to standing to light exercise (walking the aisle). Vocalization levels are typically above the range in quieter non-aircraft settings and

Table XIII. Relative Breathing Rate Enhancement Factor, r_B.[43]

ACTIVITY		RELATIVE QUANTA EMISSION RATE FACTOR
PHYSICAL INTENSITY	VOCALIZATION	
Resting	Oral breathing	1.0
	Speaking	4.7
	Loudly speaking	30.3
Standing	Oral breathing	1.2
	Speaking	5.7
	Loudly speaking	32.6
Light exercise	Oral breathing	2.8
	Speaking	13.2
	Loudly speaking	85
Moderate exercise	Oral breathing	4.3
	Speaking	20.4
	Loudly speaking	132
Heavy exercise	Oral breathing	6.8
	Speaking	31.6
	Loudly speaking	204

Table XIV. Shedding Rate Enhancement Factor, r_E.[43]

	ACTIVITY LEVEL				
AGE GROUP (yr)	SLEEP OR NAP	SEDENTARY OR PASSIVE	LIGHT INTENSITY	MODERATE INTENSITY	HIGH INTENSITY
<1	0.63	0.64	1.6	2.9	5.4
1–2	0.94	1.0	2.5	4.4	7.9
2–3	0.96	1.0	2.5	4.4	8.1
3–6	0.90	0.94	2.3	4.4	7.7
6–11	0.94	1.0	2.3	4.6	8.7
11–16	1.0	1.1	2.7	5.2	10
16–21	1.0	1.1	2.5	5.4	10
21–31	0.90	0.88	2.5	5.4	10
31–41	1.0	0.89	2.5	5.6	10
41–51	1.0	1.0	2.7	5.8	11
51–61	1.1	1.0	2.7	6.0	11
61–71	1.1	1.0	2.5	5.4	9.8
71–81	1.1	1.0	2.5	5.2	9.8
>81	1.1	1.0	2.5	5.2	10
Average	1.0	1.0	2.4	5.0	9

might range from a normal speaking level up to a loud speaking level. The activity levels will all generally be further enhanced during boarding and deplaning. Conservative values for r_B and r_E, 2.0 and 1.5, respectively, will be assumed in the following calculations. Note that if any single infectious individual were to be speaking loudly for most of the flight, then the enhancement value for the quanta shedding rate could be on the order of 10 times higher, and the resulting risk of infection could also be on the order of 10 times higher. It is not unreasonable to expect that on any given flight such an individual might be aboard, and a pragmatic (not conservative, as is this estimate) estimate of risk should account for that possibility. Further, recent observations aboard domestic flights suggests that fewer than 10% of passengers and crew are wearing masks, and they are more often surgical masks, which are approximately 50% effective, rather than N95 masks which are 90–95% effective in filtering airborne viral pathogens. Therefore, the penetration efficiency of virus-carrying particles through masks may be taken to be 0.95 for both f_e and f_i, inferring that 10% of passengers are wearing masks that are 50% effective. Substitution into Eq. 15 of the above assumed values, as follows:

$$r_{ss} = 1;\ r_E = 1.5;\ r_B = 2.0;\ B_0 = 0.288\,m^3/h;\ f_e \text{and} f_i = 0.95$$

results in the estimated number of passengers who will be infected on any given flight, $PAX_{flight,inf}$:

$$\begin{aligned} PAX_{flight,inf} &= N_{PAX}{}^2 \times P_{PAX,ill} \times \%_{pop,ill,day} \times \%_{fly} \\ &\quad \times E_{p0} \frac{0.288 \times 1.0 \times 1.5 \times 2.0 \times 0.95^2 \times D}{V \times ACH_{tot}} \\ &= \%_{pop,ill,day} \times \%_{fly} \times E_{p0} \times N_{PAX}{}^2 \frac{0.78 \times D}{V \times ACH_{tot}} \end{aligned} \quad \text{Eq. 16}$$

One can select a typical aircraft and flight parameters as follows:

- Boeing 737 cabin with dimensions: L = 30.0 m; W = 3.5 m; H = 2.2 m;
- with 189 maximum passengers and $N = 162$ typical passengers; and
- ventilation rate providing $ACH_{vent} = ACH_{tot} = 30/h$.[9]

The interior volume of the cabin (V, in Eq. 16) may be estimated from the cross-section drawing[19] of the cabin interior of a Boeing 737-200, which shows the nominal 3.5-m width and 2.2-m height. Later versions of the Boeing 737, including the 737-800, have the same interior cabin dimensions.[10] A simple estimate of the volume of air in the cabin could be obtained by assuming a rectangular cross-section of 3.5 m × 2.2 m (7.7 m^2) along the 30.0 m length, resulting in V = 231 m^3. But a more accurate estimate is obtained by omitting the volume of the overhead compartments, so that the cross-section is 3.5 m × 1.58 m + 1.16 m × 0.62 m = 6.24 m^2, resulting in V = 184 m^3. The average U.S. domestic flight duration (D, in Eq. 16) is approximately 2.5 h.[39] The average time that a passenger is in the aircraft on the ground includes: 30 min boarding (estimate); 17 min to taxi out; 9 min to taxi in; and 20 min to deplane (estimate), for a total of 76 min on the ground.[23] This will be rounded down herein from 76 min to 60 min, to be conservative.

Evaluating Eq. 16 during the average cruising time of 2.5-h aboard a Boeing 737, with 30 ACH ventilation, results in:

$$\begin{aligned} PAX_{flight,inf} &= \%_{pop,ill,day} \times \%_{fly} \times E_{p0} \times N_{PAX}{}^2 \frac{0.78 \times D}{V \times ACH_{tot}} \\ &= \%_{pop,ill,day} \times \%_{fly} \times E_{p0} \times 162^2 \times \frac{0.78 \times 2.5}{184 \times 30} \\ &= 9.27 \times \%_{pop,ill,day} \times \%_{fly} \times E_{p0} \end{aligned} \quad \text{Eq.17}$$

Eq. 17 can be evaluated for any given pathogen, where each of the remaining variables, $\%_{pop,ill,day}$, $\%_{fly}$, E_{p0}, vary depending on the pathogen and its prevalence among the population on the day of the flight. Further below, following Eq. 18 and 19, the annual average infections and deaths will be calculated for the entire U.S. commercial aircraft fleet. However, Eq. 17 can immediately be used to provide insight into the scale of the

infection risk, as follows. As will be evaluated in detail below, one can assume that $\%_{fly} = 50\%$ and $\%_{Pop,ill,day} = 0.104\%$.

The last parameter needed in Eq. 17, E_{p0}, equals 18.4 quanta/h for SARS-CoV-2. Then the result of Eq. 17 is that an estimated 0.089 passengers will become infected with SARS-COV-2 on every flight. This result incorporates the relatively low probability, 0.104%, that any given person in the population is sick on the day of the flight. Multiplying this 0.104% times 162, the average number of passengers on a flight, indicates a 17% probability that there is a passenger on any given flight who has SARS-CoV-2 during the flight. Further, if one assumes that there is one sick passenger on a flight, then the estimated number of passengers who will become infected with SARS-COV-2 on that flight is 0.089/0.17 = 0.53.

In order to evaluate the total number of annual infections transmitted aboard all U.S. commercial aircraft using Eq. 17, one needs to consider not just the 162 passengers on an average Boeing 737 flight, but rather the average 106 passengers on the roughly 10,000,000 annual U.S. flights, which include commercial aircraft of all sizes. A good assumption is that the passenger density on other commercial aircraft is comparable to that on a Boeing 737, and that the ventilation has a comparable 30 ACH. The average annual number of passengers on U.S. airlines is 798,000,000 from Table III. To prorate the estimated number of passengers who will become infected on any given 2.5-h flight aboard a Boeing 737, it is fair to estimate that if all of the 798,000,000 annual passengers on U.S. commercial flights flew aboard a Boeing 737 with 162 passengers aboard, that would require 798,000,000/106 = 7,530,000 flights ($N_{flights,ann}$). This is, of course, a bit lower than the roughly 10,000,000 annual flights reported by the FAA since the average aircraft may be smaller than a 737. For simplicity, what is desired is a reasonable U.S. average, without going through all the statistics for every type of aircraft. Then the estimated total number of passengers, $PAX_{ann,inf}$, who will become infected annually aboard U.S. commercial aircraft is given by:

$$\begin{aligned} PAX_{ann,inf} &= PAX_{flight,inf} \times N_{flights,ann} = 9.27 \times 7{,}530{,}000 \\ &\quad \times \%_{pop,ill,day} \times \%_{fly} \times E_{p0} \\ &= 69{,}800{,}000 \times \%_{pop,ill,day} \times \%_{fly} \times E_{p0} \end{aligned} \qquad \text{Eq.18}$$

The estimated total annual number of passengers, $PAX_{ann,deaths}$, who will die annually due to transmission of an infectious disease aboard U.S. commercial aircraft is then determined by the mortality rate, M, which is the ratio of the number of deaths to the number of infections, for the disease of interest:

$$\begin{aligned} PAX_{ann,deaths} &= M \times PAX_{ann,inf} \\ &= 69{,}800{,}000 \times \%_{pop,ill,day} \times \%_{fly} \times E_{p0} \times M \end{aligned} \qquad \text{Eq. 19}$$

Eq. 18 and 19 apply to the U.S. annual average infections and deaths across all commercial aircraft for an arbitrary airborne pathogen, assuming a 2.5-h cruise period of flight with 30 ACH ventilation. Rather than using the demographically weighted statistics from the epidemiological methodology above, simpler age-independent infectiousness and mortality rates will be assumed throughout the flying public in this mechanistic model of the Wells-Riley Model calculations. This maintains independence of the input assumptions between the two methodologies and simplifies the mechanistic calculations.

MECHANISTIC MODEL OF THE WELLS-RILEY FORMALISM TO ESTIMATE RESIDUAL RISK

Due to Influenza A

Using the Wells-Riley formalism developed above, one can estimate the annual number of passengers who will be infected by onboard transmission of Influenza A and estimate how many will die by inserting the appropriate values for Influenza A into Eq. 18 and 19. The average number of annual symptomatic Influenza A illnesses in the United States from 2010–2019 equals 28,300,000, or 77,500 new cases daily. As above, influenza is contagious for 5 d on average. With an average of 5 d of infectiousness, then an average of $5 \times 77{,}500 = 387{,}500$ in the population are infectious with Influenza A on any given day. That amounts to an infectious rate in the population of:

$$\%_{pop,ill,day} = \frac{77{,}500 \times 5}{330{,}000{,}000} = 0.117\%$$

The parameter, E_{p0}, that depends on the pathogen, is found equal to 18.4 quanta/h for SARS-CoV-2 and approximately equal to 4 quanta/h for Influenza A, inferred from Fig. 1 of Peng.[43] The ratio of E_{p0} of 18.4/4, which is approximately equal to 4, implies that the value for P_{indiv} [i.e., attack ratio (AR)] should be approximately four times higher for SARS-CoV-2 than for Influenza A. The corresponding ratio of AR as provided in Rafferty[45] is 1.17%/0.5% or approximately two times higher. Considering the wide range (greater than 10) of possible values for r_B and r_E, this twofold difference may be interpreted as good agreement, providing some confidence in the accuracy of Eq. 17, and in the accuracy of this methodology for order of magnitude estimates. The estimated annual number of passengers who will become infected onboard by Influenza A, from Eq. 18 is:

$$PAX_{flight,inf} = 69{,}800{,}000 \times 0.117\% \times 50\% \times 4 = 163{,}332 \quad \text{Eq. 20}$$

This is 3 times less than the epidemiological estimate from above, which is 473,814. This is a fairly good agreement, considering that the two approaches are nearly independent of each other. Possible sources of the lower estimate from the present Wells-Riley formalism of Eq. 20 include:

- The assumed 3.0 times enhancement of breathing rates ($r_E \times r_B = 1.5 \times 2.0 = 3.0$) due to talking and activity level of the passengers could be higher, increasing the Wells-Riley calculation; and
- The value $B_0 = 4$ quanta/h is not well known for Influenza A and may be higher, also increasing the Wells-Riley result.

The annual mortality in the United States due to Influenza A is 34,700,[48] so the average mortality rate is 34,700/28,300,000 = 0.12%. From Eq. 19, the estimated total number

of passengers who will die annually due to transmission of Influenza A aboard U.S. commercial aircraft while cruising is:

$$PAX_{ann,deaths} = M \times PAX_{ann,inf} = 0.12\% \times 163,332 = 196 \quad \text{Eq. 21}$$

Repeating the above calculations for the 1-h time on the ground, with 15 ACH ventilation (conservative), another 156 deaths accrue annually due to transmission of Influenza A aboard U.S. commercial aircraft while the aircraft is on the ground with passengers aboard. Combining the cruise and ground portions of each flight, the estimated total number of passengers who will die annually due to transmission of Influenza A aboard U.S. commercial aircraft, per the Wells-Riley formalism, is:

$$PAX_{ann,deaths} = 196 + 156 = 352 \quad \text{Eq. 22}$$

Unlike the epidemiological methodology above, the present mechanistic model of the Wells-Riley formalism makes no assumption regarding secondary infections and deaths in the general population who are infected by those who were infected onboard. In total 352 deaths/year are due to transmission of Influenza A aboard U.S. commercial aircraft. This total results from statistics from the 2010–2019 period and so are independent of the COVID pandemic. From the epidemiological methodology above, the annual deaths, including those from secondary infections in the general population who were infected from the primary infected passengers, was somewhat higher at 599.

Due to SARS-CoV-2

Only a few of the variables in the calculations for risk of Influenza A infection above need to be modified for the risk of SARS-CoV-2 infection: E_{p0}, % of passengers who are infectious, and the mortality rate. By fitting epidemiological data from 12 well-documented outbreaks of SARS-CoV-2 as presented in Peng,[43] where P_{indiv}, D, V, and ACH_{tot} were documented, the best fit to the data established that E_{p0} = 18.6 quanta/h for SARS-CoV-2, which is approximately 4 times higher than that for Influenza A, i.e., the average rate of exhalation of infectious doses is much higher for those infected with SARS-CoV-2 than for those infected with Influenza A. Simply stated, SARS-CoV-2 is more infectious. The COVID-19 mortality rate in the United States for the 12 mo ending in March 2023 and also for the 20-mo period February 2020 through September 2021 is approximately 1.0%.[15] For the 20-mo period February 2020 through September 2021, there were approximately 71,100 daily average new cases of COVID-19, and for the 12 mo ending in March 2023, there were approximately 65,700 daily average new cases. Therefore, the two periods may both be estimated by assuming the average of those two figures, which is 68,400 daily new cases, and a 1% mortality rate. With an average of 5 d of infectiousness, then an average of $5 \times 68,400 = 342,000$ in the U.S. population were infectious with SARS-CoV-2 on any given day during that period. That amounts to an infectious rate in the population of:

$$\%_{pop,ill,day} = \frac{68,400 \times 5}{330,000,000} = 0.104\%$$

Again, the percentage of passengers who elect to fly while infectious is assumed to be $\%_{fly}$ = 50%. Substituting the above values for COVID-19 into Eq. 18, the estimated total number of passengers, $PAX_{ann,inf}$, who became infected with COVID-19 annually while cruising aboard U.S. commercial aircraft during the high-pandemic range of February 2020 through September 2021, and for the 12 mo ending in March 2023, is:

$$PAX_{ann,inf} = 69,800,000 \times 0.104\% \times 50\% \times 4 = 675,106 \quad \text{Eq. 23}$$

Substituting the 1% mortality for COVID-19 into Eq. 19, the estimated total number of passengers, $PAX_{ann,deaths}$, who died annually due to becoming infected with COVID-19 while cruising during the high-pandemic range of February 2020 through September 2021, and for the 12 mo ending in March 2023, aboard U.S. commercial aircraft is:

$$PAX_{ann,deaths} = M \times PAX_{ann,inf} = 1\% \times 675,106 = 6,751 \quad \text{Eq. 24}$$

As with Influenza A, there are an additional 80% deaths resulting from the average 60 min on the ground with 15 ACH ventilation, adding 5400, for a total of 12,151. As opposed to the results for Influenza A, which were lower, this is approximately 2 times higher than the epidemiological estimate for secondary deaths from above, which is 6652. Again, this is good agreement, considering that the two approaches are nearly independent of each other, and accounting for the possible sources of the uncertainties in the present Wells-Riley formalism mentioned above relative to Eq. 20.

The results for infections, deaths, and economic burden from both methodologies for both diseases, Influenza A and COVID-19, are summarized in **Table XV**. In summary, the annual deaths due to transmission of Influenza A aboard U.S. commercial aircraft based on data from 2010–2019 are:

- 599 using the epidemiological methodology based on data from February 2020 through September 2021; and
- 352 using the mechanistic model of the Wells-Riley methodology, based on data from March 2022 through March 2023.

In summary, the annual deaths due to transmission of SARS-CoV-2 aboard U.S. commercial aircraft are:

- 8720 using the epidemiological methodology based on data from February 2020 through September 2021; and
- 12,151 using the mechanistic model of the Wells-Riley methodology based on data from February 2020 through September 2021, as well as for the 12 mo ending in March 2023.

Given the nearly independent approaches of the epidemiological and mechanistic model estimates, and the potential approximate factor of 2 precision of some of the input variables, one might reasonably expect the results between the two to agree within a range no better than approximately a factor

Table XV. Infections, Deaths, and Economic Burden from Epidemiological Methodology for Both Diseases, Influenza A and COVID-19, for the Analysis Period April 2022 Through March 2023 (Ongoing).

					ECONOMIC BURDEN ($ BILLION)			
PATHOGEN	ANALYSIS PERIOD	TYPE OF CASE	INFECTIONS	DEATHS	TOTAL	MEDICAL	INFECTIONS	DEATHS
Influenza A	2010–2019	Primary	473,814	38	2.8	0.6	163,332	352
		Secondary	473,814	599			-	-
COVID-19	2/20 to 9/21	Primary	1,058,334	2067	818	24.3	974,852	9748
		Secondary	1,058,334	10,000			-	-
Totals			3,064,296	12,704	821	24.9	1,138,184	10,100

of 2–5. Furthermore, in order to determine the risk–benefit of the application of UV-C to mitigate these disease burdens, or to comprehend the magnitude of the burden, this approximate 2–5 times range of uncertainty is not significant. It is therefore reasonable to express a best estimate of these results, approximately, as follows. There is an estimated ongoing annual average, post-pandemic, of on the order of 3000 deaths due to transmission of these two diseases combined aboard U.S. commercial aircraft. Even as the COVID-19 pandemic becomes endemic, longer term, with approximately 40,000 deaths/year (comparable to Influenza A), the combined annual deaths due to transmission of SARS-CoV-2 and Influenza A aboard U.S. commercial aircraft is still estimated to be on the order of 2000 or more. Further, infections and deaths due to onboard transmission of other airborne diseases in the United States, e.g., pneumonia, RSV, and others, are not negligible, and are comparably well avoided using UV-C, as are SARS-CoV-2 and Influenza A infections. Of even greater importance than the waning endemic COVID-19, the "next" airborne pandemic could be substantially mitigated by having UV-C operational in advance, as demonstrated below, since UV-C is known to be highly efficacious in inactivating airborne pathogens of all kinds.

UV-C DISINFECTION EFFICACY IN AIR EXPRESSED AS EQUIVALENT AIR CHANGES PER HOUR

The standard metric used to quantify an environmental air control other than ventilation is equivalent air changes per hour (eACH, sometimes called ACH_{eq}), which quantifies the ability of an environmental control (e.g., UV) to kill or inactivate an airborne microorganism in addition to the rate at which mechanical ventilation physically removes the airborne microorganism from a space, as measured in ACH. The eACH is a measure of the UV efficacy that can be obtained using decay model experimental conditions in a well-mixed space. The eACH for different microorganisms will vary according to the relative susceptibility of the target pathogen to the wavelength of UV that is applied.[56] Therefore, whereas the ACH obtained by mechanical ventilation is usually independent of the type of pathogen, the eACH obtained by UV disinfection varies in proportion to the susceptibility of the pathogen to the applied UV-C. Fortunately, most airborne pathogens of interest are highly susceptible to UV-C irradiation.

The quantitative impact of increasing ACH can be evaluated most simply under two common situations. First is the release of airborne pathogens at a single point in time (transient analysis), and the second is a constant release of airborne pathogens over time (steady-state analysis). In the first situation, under ideal conditions in a room where droplet nuclei (exhaled respiratory particles) are released at a single point in time, mechanical room ventilation reduces the number of droplet nuclei in the room in a logarithmic fashion when plotted against time. In the absence of mechanisms to introduce new pathogens into an indoor space, and assuming uniform spatial distribution of pathogens throughout the space (i.e., well-mixed air), the concentration of pathogens, n(t), in air will decay vs. time due to several different mechanisms (the components of R, below)[8,24,34]:

$$n(t) = n_0\, e^{-R\times t} \qquad \text{Eq. 25}$$

The pathogen removal rate, R, is given by:

$$R = ACH_{vent} + ACH_{UV} + ACH_{other} + \kappa + \lambda \qquad \text{Eq. 26}$$

where: t = time (h); N = virus concentration (quanta/m^3), where a quantum is defined as the dose of airborne droplet nuclei required to infect 63% of susceptible individuals; n_0 = initial virus concentration (quanta/m^3) at t = 0; ACH_{xx} = inactivation rate (h^{-1}) from an air disinfection system such as ventilation, filtration, UV, or other inactivation mechanism; κ = natural viral inactivation rate (i.e., its natural "death" rate, λ_{dec} in Eq. 1) = 0.63 h^{-1} for SARS-CoV-2 in still air at 25°C;[54] and λ = deposition rate (h^{-1}, λ_{dep} in Eq. 1) onto surfaces due to gravitational settling and surface adsorption.

Studies by Miller's and Kujundzic's groups[33,36] examined the relationship between an Upper-Room Ultraviolet Germicidal Irradiation (UR-UVGI) system, portable air cleaners, and HVAC ventilation rates of 0 and 6 ACH, and found that, as long as the air was well-mixed, the particle removal rates of the three systems were additive.[56] In other words, one can expect that the supplementation of mechanical ventilation with UV-C disinfection will result in a composite disinfection rate equal to the sum of the two separate rates.

Note that one air change does not imply that 100% of the air in the space has been replaced; rather, it means that 63% ($1 - e^{-1}$) of the air in the space has been replaced, assuming a well-mixed space. That is because the air injected into the

space does not push the ambient air out of the space like a piston, but rather the injected air mixes with the ambient air, and the mixture is exhausted from the space by the ventilation system. The exhausted air comprises both the initial ambient air and the injected air during each flushing of the volume of air. If the pathogen removal rate (R) is $1\,h^{-1}$, the airborne viral concentration is reduced by 63% after 1 h and the remaining 37% of the concentration is reduced by another 63% in the next hour, resulting in an 86% reduction after 2 h. Similarly, the airborne pathogen concentration is reduced by 95% and 98% after 3 and 4 h, respectively. In this formalism, eACH due to UV-C irradiation contributes to the total virus removal rate, R, in the same way as the other virus-removal mechanisms, so that UV inactivation may be expressed by each value for direct comparison with the other virus-removal systems. In this way, any addition to R from the eACH of a UV disinfection system contributes to a multilayered infection-control strategy.

Note that the sum of natural decay, κ, and settling onto surfaces, λ, is approximately 1 eACH for SARS-CoV-2. If a UV system is designed to enhance the removal of pathogens significantly beyond the rate of natural removal mechanisms, i.e., eACH is much greater than 1, then for simplicity, the natural removal mechanisms, κ and λ, may be ignored as components of R in Eq. 26. Also ignoring contributions from ACH_{other}, and considering only the air disinfection contributions from ventilation and UV, Eq. 25 simplifies to:

$$n(t) = n_0\, e^{-(ACH_{vent} + ACH_{UV}) \times t} \qquad \text{Eq. 27}$$

Therefore, the total equivalent AER in an environment having both traditional ventilation and UV as the only supplemental environmental control is approximately the sum from ventilation and UV:

$$R = ACH_{total} \cong ACH_{vent} + ACH_{UV} \qquad \text{Eq. 28}$$

Since UV is the only air disinfection process other than ventilation (ACH_{vent}), from this point forward in this analysis, one may use the terms eACH and ACH_{UV} interchangeably. For example, an aircraft ventilation system providing 15–30 ACH_{vent} of fresh or filtered air may be supplemented by a UV system that provides an additional 30 eACH for a total of 45–60 ACH_{total} to the space. Thereby, the rate of total reduction of pathogens in the air will be 2–3 times as fast with the combined ventilation and UV vs. with ventilation alone. Although some aircraft ventilation is quoted as high as 35 ACH_{vent}, a typical value of 30 ACH_{vent} will be used in the calculations herein.

Pathogen concentrations vs. time for ACH values of interest to airlines, plotted from Eq. 27 for various values of R = ACH_{tot}, are shown in **Fig. 2**. The lowest two values, ACH_{vent} = 15 and 30, pertain to the range of values typically found in commercial aircraft. The highest two values represent the addition of a supplemental 30 eACH from UV to the two filtered air ventilation rates. In fact, with present technology, 60–120 eACH may be achieved with UV-C in an aircraft cabin. Even though the enhancement in ACH due to UV is only increased by a factor of two to three times, it appears in the exponent of Eq. 27, so that as the pathogen reduction rate is compounded over time, the cumulative benefit of the higher eACH grows from on the order of five times lower concentration after 3 min, to on the order of 20 times lower at 6 min, to on the order of 100 times lower at 9 min, and to on the order of 500 times lower at 12 min (0.2 h on the x axis).

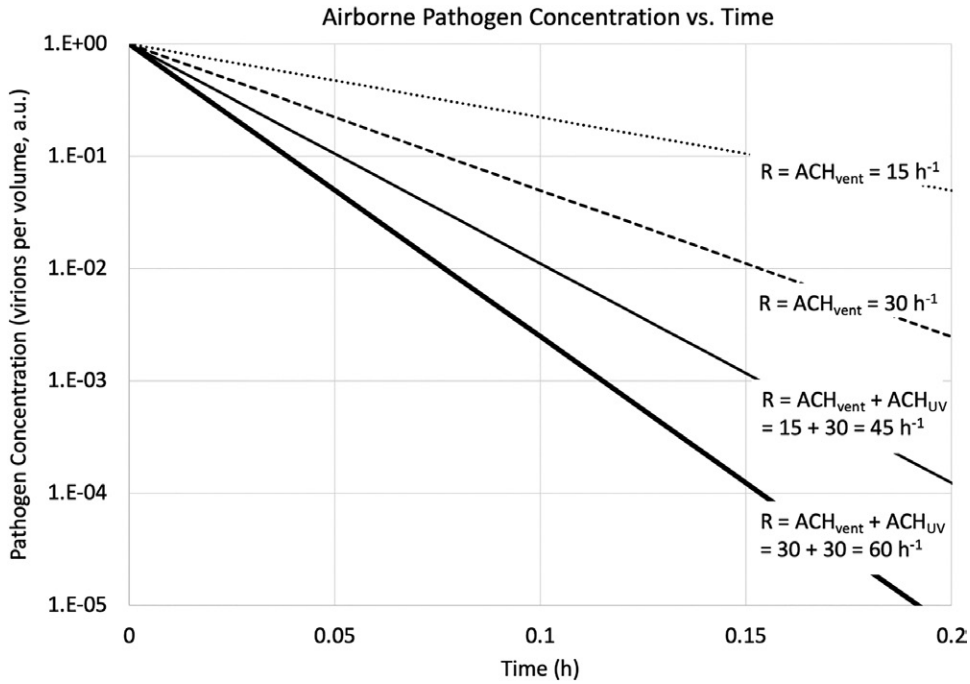

Fig. 2. Pathogen concentration vs. time for ACH_{tot} values of interest for airlines.

Of significant importance, the greatest risk of airborne infection occurs when the pathogen concentration greatly exceeds that required to transmit the disease (e.g., from a super spreader). If the concentration greatly exceeds that required to infect 50% of the occupants, then the reduction in concentration required to reduce the risk of any one occupant being infected may be on the order of 100 times greater or more, relative to a much lower pathogen concentration, as will be shown further below. Given that this scenario with a very high pathogen concentration and very high level of risk will have an outsized impact on overall risk in airlines compared to a scenario with lower concentration and lower risk of infection, it is critically important that the baseline ACH of 15–30 from ventilation be supplemented by at least 2–4 times, or much more, to significantly reduce the likelihood of infections in scenarios with high pathogen concentrations.

As mentioned above, there are two distinct methods to quantify the reduction in pathogen concentration due to an air disinfection method in an indoor space.

- The first, evaluated above, is to quantify the transient rate of decay of pathogen concentration following a one-time introduction of pathogens into the space with and without the subject air disinfection method activated.
- The second, evaluated below, is to quantify the ratio of equilibrium pathogen concentration during a continuous and constant generation of airborne pathogens into the space, with and without the subject air disinfection method activated.

When airborne pathogens are introduced into a space at a constant continuous rate R_e by N_{inf} infectious individuals, the time-dependent pathogen concentration, n(t), is as follows, assuming well-mixed air and spatial uniformity throughout the space:

$$n(t) = \frac{R_e \times N_{inf}}{R \times V} + \left(n_0 - \frac{R_e \times N_{inf}}{R \times V} \right) \times e^{-R \times t} \qquad \text{Eq. 29}$$

where: R = pathogen removal rate (h^{-1}); R_e = emission rate (h^{-1}) of pathogens exhaled per hour per infectious subject; N_{inf} = number of infectious individuals in the space; V = volume of the space (m^3); and n_0 = initial pathogen concentration.

In equilibrium, at $t = \infty$, the exponential factor goes to zero, so that for a single infectious individual ($N_{inf} = 1$), Eq. 29 simplifies to the equilibrium value of $N = n_\infty$, as expected:

$$n_\infty = \frac{R_e}{R \times V} \qquad \text{Eq. 30}$$

Then, from Eq. 30, considering ventilation only (R = ACH_{vent}), the equilibrium pathogen concentration for a given R_e and V is:

$$n_{\infty,vent} = \frac{R_e}{ACH_{vent} \times V} \qquad \text{Eq. 31}$$

With the supplementation of ACH_{UV}, in addition to ventilation, the equilibrium pathogen concentration for a given R_e and V with ventilation rate, ACH_{vent}, supplemented by UV having an inactivation rate ACH_{UV}, is:

$$n_{\infty,vent+UV} = \frac{R_e}{(ACH_{vent} + ACH_{UV}) \times V} \qquad \text{Eq. 32}$$

And the ratio, ρ, of equilibrium pathogen concentrations, with and without the addition of UV disinfection, from Eq. 31 and 32 is:

$$\rho \equiv \frac{n_{\infty,vent+UV}}{n_{\infty,vent}} = \frac{ACH_{vent}}{ACH_{vent} + ACH_{UV}} = \frac{15}{45} = \frac{1}{3} \qquad \text{Eq. 33}$$

Following the example provided above, an aircraft ventilation system providing 15–30 ACH of fresh or filtered air, when supplemented by a UV system that provides an additional 30 eACH, provides a total 45–60 eACH to the space. Therefore, the equilibrium airborne pathogen concentration in Eq. 31 is reduced by a factor of 2–3 with UV-C vs. without it. If the aircraft ventilation system provides only 5–10 ACH, for example, when grounded, then the reduction of equilibrium airborne pathogen concentration with and without UV ranges from a factor of 6–12 times. If the risk of disease transmission is enhanced due to low ACH_{vent} while a grounded aircraft is occupied, then the supplementation of ACH_{UV} is especially effective in reducing the risk while grounded.

It will be quantified later in this document that 30 ACH (for example) of aircraft ventilation reduces the risk of infection to some residual (unmitigated) level, and that the addition of UV in a multilayered risk mitigation approach makes a significant additional contribution to risk reduction, well below the residual risk provided by ventilation alone. The benefit of that additional risk reduction afforded by UV disinfection will be quantified below in human and financial terms and weighed against the risks due to the incremental UV dose to an individual.

For the case when $ACH_{vent} = 0$, such that UV is the only mechanism of pathogen inactivation, then Eq. 27 simplifies to:

$$n(t) = n_0 \, e^{-eACH \times t} \qquad \text{Eq. 34}$$

For UV disinfection of air, the infectious pathogen inactivation rate due to UV disinfection, eACH (ACH_{UV}), in Eq. 26, has been shown to be given by eACH = Z × E.[2] Including the conversion from hours to seconds, eACH can be calculated from Eq. 35 below:

$$\text{eACH}\left(h^{-1}\right) = 3600 \left(\frac{s}{h} \right) \times Z \left(\frac{m^2}{J} \right) \times E \left(\frac{W}{m^2} \right) \qquad \text{Eq. 35}$$

where Z ($m^2 \cdot J^{-1}$) is the UV susceptibility constant for the pathogen, sometimes referred to as the UV rate constant, k, ($m^2 \cdot J^{-1}$)[32]; E is the UV fluence ($W \cdot m^{-2}$) assumed to be uniform throughout the space; and $1\,W = 1\,J \cdot s^{-1}$.

Another useful term quantifying the application of UV disinfection is the UV dose, D, defined as: D ($J \cdot m^{-2}$) ≡ 3600

$(s \cdot h^{-1}) \times E\ (W \cdot m^{-2}) \times t\ (h)$. Substituting Eq. 35 into Eq. 34, along with the definition above of dose, D, yields:

$$\frac{n(t)}{n_0} = e^{-3600 Z \times E \times t} = e^{-Z \times D} \qquad \text{Eq. 36}$$

The UV dose, D ($J \cdot m^{-2}$), is typically identified as the flux density ($J \cdot m^{-2}$) of UV required to inactivate a given percentage of airborne pathogen concentration. For example, a D_{90} dose refers to the flux density ($J \cdot m^{-2}$) of UV at which the initial pathogen concentration, n_0, is reduced by 90%; a D_{99} dose refers to the flux density ($J \cdot m^{-2}$) of UV at which the initial pathogen concentration, n_0, is reduced by 99%; and so on.

The dose, D_{90}, at which the initial pathogen concentration, n_0, is reduced by 90% is found by solving Eq. 36 for $\frac{n(t)}{n_0} = 0.10$:

$$0.1 = e^{-Z \times D_{90}} \Rightarrow D_{90} = \frac{-ln(0.1)}{Z} = \frac{2.30}{Z} \qquad \text{Eq. 37}$$

For example, Z for SARS-CoV-2 in air is 0.377 $m^2 \cdot J^{-1}$,[32,55] so that $D_{90} = 6.1\ J \cdot m^{-2}$. If the uniform UV fluence in the space is 0.01 $W \cdot m^{-2}$, every hour the cumulative UV Dose is 36 $J \cdot m^{-2}$.

The time, t_{90}, to achieve 90% inactivation of the initial pathogen concentration is defined by solving Eq. 36 at $t = t_{90}$:

$$\frac{n(t_{90})}{n_0} \equiv 0.10 = e^{-3600 Z \times E \times t_{90}} = e^{-Z \times D_{90}} \qquad \text{Eq. 38}$$

Solving Eq. 38 for SARS-CoV-2 in air with a uniform UV fluence in the space equal to 0.01 $W \cdot m^{-2}$:

$$t_{90}(h) = \frac{D_{90}\left(\frac{J}{m^2}\right)}{3600 \times E\left(\frac{W}{m^2}\right)} = \frac{6.1}{3600 \times 0.01} = \frac{1}{6} h \qquad \text{Eq. 39}$$

Note that the time, t_{90}, to disinfect 90% of the airborne pathogens increases in proportion to D_{90} (inversely proportional to the UV susceptibility of the pathogen, Z), and decreases in proportion to the UV irradiance, E, i.e., higher UV irradiance provides shorter disinfection time. Eq. 39 has been evaluated above for the case of $D_{90} = 6.1\ J \cdot m^{-2}$, and $E = 0.01\ W \cdot m^{-2}$, resulting in t_{90} equal to 10 min. Therefore, the application of a very low irradiance level of UV-C at 0.01 $W \cdot m^{-2}$ (10 $mW \cdot m^{-2}$) inactivates 90% of airborne SARS-CoV-2 virus in only 10 min, and 99% in 20 min.

UV-C SUSCEPTIBILITY CONSTANT, K, IN AIR FOR SARS-COV-2 AND INFLUENZA

Inactivation rates of pathogens subject to 254 nm UV-C have been studied for decades, since 254 nm is the primary wavelength emitted by low-pressure mercury (Hg) lamps, which have been the mainstay light source for disinfection for decades prior to the recent advent of UV-C LEDs. A database of D_{90} values for hundreds of pathogens in air and water, and on surfaces is provided in published manuals and guidelines.[32] A subset, including only viruses and only in air, of Kowalski's dataset[32] is shown in **Table XVI**. A conclusion from Table XVI is that a typical value for D_{90} for viruses in air at 254 nm is on the order of 10 $J \cdot m^{-2}$ (the value for SARS-CoV-2 is 6 $J \cdot m^{-2}$, and for Influenza A is 19 $J \cdot m^{-2}$).

UV-C susceptibility data for airborne viruses at wavelengths other than 254 nm have historically been sparse, but have been emerging recently from studies using excimer lamps at 222 nm and UV-C LEDs at a range of UV-C wavelengths above and below 254 nm.[34] The results of one recent study performed in aqueous solution (not airborne) demonstrate that there is generally a twofold decrease in susceptibility from 222 nm to 282 nm in aqueous solution.[34] The notable exception is the extremely high susceptibility of Phage phi 6 at 222 nm, which is approximately 12 times higher than that at 254 nm. Similar results were reported by Beck[7] in 2015 using a tunable UV laser for various pathogens, again in aqueous solution. Similar results were further reported by Handler in a 2019 review of four different sources of data for the bacterium *Bacillus subtilis* in air, vacuum, and water.[26] The overall conclusion from the 13 different datasets from these 3 references is that the UV-C susceptibility of several pathogens, including bacteria and viruses, in aqueous and airborne media, tend to peak at around 265 nm, falling off slightly at both shorter and longer wavelengths, then falling off dramatically above 280 nm, and increasing dramatically (for some pathogens) below 240 nm. Of relevance to this publication, the relatively flat dependence of UV-C susceptibility between 240–280 nm infers relative confidence (within a factor of 2) that susceptibility data from decades of research at 254 nm apply to all wavelengths between 240–280 nm. D_{90} values in air are listed in **Table XVII** for common pathogens of interest.

EXPLANATION FOR THE UNEXPECTEDLY HIGH RESIDUAL RISK OF AIRBORNE INFECTIONS IN AIRCRAFT CABINS

In general, airline companies and regulators have historically asserted that passengers are very safe against transmission of

Table XVI. Summary of Dose Data at 254 nm UV-C for 90% Inactivation (D_{90}) of Viruses in Air.[32]

VIRUS	D_{90} ($J \cdot m^{-2}$)
Adenovirus	44
Bacteriophage MS2	12
Coliphage T7	8
Coliphage fX-174	3
Coronavirus	6
Coxsackievirus	21
Influenza A	19
Phage phi 6	6
Sindbis virus	22
Vaccinia virus	4
Geometric mean	10

Table XVII. D_{90} Values for Common Pathogens of Interest.

PATHOGEN	TYPE	D_{90} IN AIR ($J \cdot m^{-2}$)
SARS-CoV-2	Virus	6
Mycobacterium tuberculosis	Bacteria	5
S. aureus (e.g., Methicillin-resistant *S. aureus*, MRSA)	Bacteria	5
Coronavirus (some common colds)	Virus	6[48]
Pathogens responsible for pneumonia: *S. aureus*, *K. pneumoniae*, *P. aeruginosa*, *S. pneumoniae*	Bacteria	6
Escherichia coli	Bacteria	8
Influenza A	Virus	19
Adenovirus	Virus	44
Candida auris	Fungus	on the order of 100–500
Clostridioides difficile	Bacterial spore	on the order of 100–500

airborne disease due to the extremely high ventilation rate in a typical aircraft cabin. Therefore, the results of the calculations herein (i.e., on the order of 10,000 annual deaths due to SARS-CoV-2 and Influenza A transmitted aboard U.S. commercial flights) may be unexpected for the FAA, airline carriers, and aircraft manufacturers. These high mortality results may perhaps be unexpected because the detailed calculations, based on statistically significant databases, have only recently been published. Statistically significant data, especially for attack rate, had not been available until very recently.[45] To provide perspective to these perhaps unexpected results, one needs to get beyond the assertion that the 15–30 ACH_{vent} on airlines is much higher than in terrestrial settings and, therefore, makes the aircraft cabin very safe in comparison. That assertion breaks down due to the extremely high volume-density of passengers (and crew), e.g., 162 passengers in a volume of 184 m^3 = 0.7 people $\cdot$ m^{-3}. Compare that with a typical density of 10 people in a crowded conference room (3 m × 5 m × 8 m = 120 m^3) of 0.08 people $\cdot$ m^{-3}. Due to the 10 times higher volume-density of people in the aircraft cabin vs. the conference room, the aircraft cabin will need 10 times more ventilation to provide comparable clean air to any given passenger as any person in the conference room. If the conference room has an ACH_{vent} value of 6, as recommended by the CDC, then the aircraft would need an ACH_{vent} of 60 to be comparably as safe as a crowded conference room. However, this consideration is limited to the infection risk for any given individual. In contrast, the risk that any individual in a given setting will be infected is further multiplied by the number of susceptible individuals in that setting, as below.

From Eq. 16, repeated below, the estimated number of passengers who will become infected on any given flight, $PAX_{flight,inf}$, is:

$$PAX_{flight,inf} = \%_{pop,ill,day} \times \%_{fly} \times E_{p0} \times {N_{PAX}}^2 \frac{0.78 \times D}{V \times ACH_{tot}} \quad \text{Eq.16}$$

The denominator in Eq. 16, $(V \times ACH_{tot})$, can also be defined as the airflow rate (AF), measured in $m^3 \cdot h^{-1}$ or $ft^3 \cdot m^{-1}$ (cfm):

$$\begin{aligned} AF(cfm) &\equiv V\left(m^3\right) \times \frac{35.3\, ft^3}{m^3} \times \frac{ACH_{vent}\left(h^{-1}\right)}{60(min/h)} \\ &= 0.59\, V\left(m^3\right) \times ACH_{vent}\left(h^{-1}\right) \end{aligned} \quad \text{Eq. 40}$$

so that:

$$V\left(m^3\right) \times ACH_{vent}\left(h^{-1}\right) = 1.70\, AF(cfm)$$

Then Eq. 16 can be rewritten as:

$$\begin{aligned} PAX_{flight,inf} &= \%_{pop,ill,day} \times \%_{fly} \times E_{p0} \\ &\quad \times {N_{PAX}}^2 \frac{0.78 \times D}{1.70\, AF(cfm)} \\ &= \%_{pop,ill,day} \times \%_{fly} \times E_{p0} \times {N_{PAX}}^2 \times 0.46 \frac{D}{AF(cfm)} \end{aligned} \quad \text{Eq. 41}$$

In Eq. 41, the first three parameters are determined by the pathogen of interest, while the last three parameters, N_{PAX}, AF, and D, are determined by the aircraft and the flight parameters. The last three parameters, which are independent of the choice of pathogen, reveal the relationship for the risk of infection as a function only of the ventilation (or air disinfection) system and the number of occupants:

$$PAX_{flight,inf} \propto {N_{PAX}}^2 \frac{D}{AF} \propto N_{PAX} \times \frac{N_{PAX}}{AF} \quad \text{Eq. 42}$$

The scaling relationship of Eq. 42 applies equally to an aircraft cabin as it does to any terrestrial setting (e.g., a classroom or a restaurant).

Eq. 42 reveals the largely unrecognized challenge for air disinfection inside the aircraft cabin. As asserted by the airline industry, aircraft ventilation provides a very high 30 ACH_{vent}, which when applied to the volume of the Boeing 737 cabin, provides an impressively high 3345 cfm:

$$\begin{aligned} AF(cfm) &= 0.59\, V\left(m^3\right) \times ACH_{vent}\left(h^{-1}\right) = 0.59 \times 189 \times 30 \\ &= 3345\, cfm \end{aligned}$$

Even when the AF for the Boeing 737 is normalized to the number of passengers, it is a remarkably high value:

$$\frac{AF}{N_{PAX}} = \frac{3257}{162} = 20.1\, cfm/PAX$$

This value of 20.1 cfm/PAX compares favorably with the 2019 ASHRAE standard of 15 cfm/person and the recommendations of the World Health Organization (WHO), updated during the COVID-19 pandemic to 21.2 cfm/person for non-healthcare facilities, but is far lower than the WHO recommendation of 127 cfm/person for healthcare facilities.[31]

However, the largely unrecognized challenge for air disinfection inside the aircraft cabin from Eq. 42 is the additional factor

of N_{PAX} that further increases the risk of airborne infection onboard, simply in proportion to the higher probability of having an infectious passenger onboard. Of course, this proportionality of risk to N_{PAX} depends on the assumption that any susceptible passenger may be infected by any infectious passenger regardless of their relative locations inside the cabin, which requires that transmission be primarily due to migration of aerosols throughout the cabin, rather than the formerly believed primary transmission by large droplets (the 6-ft rule) or by fomites (surface contamination). This assumption has been firmly supported by several well-documented cases of aerosol transmission of SARS-CoV-2 and Influenza A aboard aircraft. Rafferty statistically summarizes all qualifying publications through 2023 that provide contact tracing of airborne diseases aboard aircraft with the following conclusion confirming that susceptible passengers throughout the cabin may be infected by an infectious passenger located more than 2 rows and 2 seats away: "*Overall, in the 46 investigations where proximity to the index case was reported on, 48.7% (94/193) of reported secondary cases occurred outside of the 2×2 seating area around the index case.*"[45]

The degree to which the risk of airborne disease transmission aboard aircraft is due to the excessively high number of passengers relative to the air ventilation of the aircraft cabin is demonstrated in **Table XVIII**, which shows quantitatively why the aircraft cabin carries so much higher risk of airborne disease transmission than any terrestrial setting.

The Boeing 737 aircraft cabin (and comparably ventilated and populated aircraft cabins) are favorable on the measures of ACH and AF, whereby industry claims assure the public of the safety of cabin air. Indeed, the 30 ACH during cruising exceeds the ACH of every typical terrestrial setting, even the 18 ACH recommended by the WHO during COVID-19 for a hospital operating room. This comparison has been emphasized by the airline industry as evidence of extremely well disinfected air aboard aircraft in several public-facing airline documents such as the 2020 USTRANSCOM report.[50] However, when AF is normalized to the number of occupants, AF/PAX, the Boeing 737, while comparable, is not as high as any of the terrestrial settings and is on the order of 10 times lower than the hospital OR. This makes it clear on an intuitive level that the high ACH in the aircraft cabin is not high enough to overcome the extreme occupancy load in the cabin, relative to typical terrestrial settings. However, there is a further nonintuitive factor in the extreme risk of airborne disease transmission aboard aircraft due to the extra N_{PAX} factor in the right-most column of Table XVIII, N_{PAX}^2/AF, which is the column that compares relative risk of airborne transmission according to Eq. 42. The aircraft cabin value of N_{PAX}^2/AF is 10–50 times higher than that of a crowded restaurant or conference room, and more than 100 times higher than that of the hospital OR, for which the USTRANSCOM report claims lower risk in aircraft[50]—a misleading factor of 100 in its message to the public.

The most concerning aspect of this 10–100 times insufficiency in ventilation in the aircraft cabin is that it is not possible to increase the aircraft cabin ventilation by the necessary 10 times or more beyond the existing 30 ACH due to energy load, mechanical design, noise, and draft discomfort. The factor of 10 or more deficit in air disinfection in the aircraft cabin must be bridged by a supplemental air disinfection method. UV-C disinfection is the only technology presently available that can provide up to 10 times or more of supplemental eACH safely, economically, and comfortably.

REDUCTION IN RISK OF INFECTION DERIVED FROM THE WELLS-RILEY EQUATION

As discussed above, air disinfection by UV irradiance can be quantitatively compared to air disinfection by ventilation by introducing an eACH for UV disinfection:

$$eACH\left(h^{-1}\right) = 2.30 \times E\left(J/h - m^2\right) / D_{90}\left(J/m^2\right) \qquad \text{Eq. 43}$$

where E is the UV irradiance averaged throughout the volume of the cabin and D_{90} is the UV dose required to achieve 90% inactivation of a pathogen in air. Note that in Eq. 43, the usual units for E, which are $(W \cdot m^{-2})$, are converted to $(J/h\text{-}m^2)$, by substituting $1\,W = 1\,J \cdot s^{-1}$ and $3600\,s = 1\,h$.

If the irradiance is incident upon occupants, then the Exposure Limit (EL; also called Threshold Limit Value, TLV) must not be exceeded. For example, D_{90} for SARS-CoV-2 in air is approximately $6\,J \cdot m^{-2}$.[55] The irradiance, E, when operated at the allowable EL for 265 nm is $1.2\,mW \cdot m^{-2} = 4.3\,J/h\text{-}m^2$. So, the theoretical maximum allowed for eACH without exceeding the EL is

$$eACH = 2.30\frac{4.32\left(\frac{J}{h-m^2}\right)}{6\left(\frac{J}{m^2}\right)} = 1.6/h$$

Table XVIII. Comparison of Air Disinfection Parameters in a Boeing 737 Cabin vs. Terrestrial Settings.

GENERAL SETTING	SETTING	TIME (h)	V (m^3)	*N* (#)	*N*/V (#/m^3)	ACH (/h)	AF (cfm)	AF/PAX (cfm/person)	$N_{PAX} \times N_{PAX}/AF$
737 Aircraft	Boarding & De-planing	1.0	184	162	0.9	15	1628	10	16
	Cruising	2.5				30	3257	20	8
Terrestrial	Restaurant	2	280	20	0.07	3	496	25	0.81
	Conference Room	1	120	10	0.08	4	283	28	0.35
	U.S. Home	4	90	3	0.03	2	106	35	0.08
	Hospital OR	2	72	6	0.08	18	765	127	0.05

PAX: passengers.

The eACH can be enhanced by approximately 3× by optically tailoring the intensity distribution in the occupied space, whereby the fluence onto an airborne pathogen may be incident from all spherical directions, while the irradiance onto the skin or eyes that determines the EL is limited to the 80° acceptance angle of the detector, per ICNIRP guidelines.[2,27] Even with practical optical enhancement, eACH will generally be limited to approximately 5/h at 265 nm[2].

The eACH can be increased very effectively by using shorter UV-C wavelengths, since the allowed EL rises sharply especially below 240 nm, as shown in **Fig. 3**. New guidelines[1] published by the American Conference of Governmental Industrial Hygienists (ACGIH) in 2022 are poised to significantly increase the allowed EL below 240 nm based on decades-old evidence of the greatly reduced penetration depth of UV-C into skin and eyes with decreasing wavelength. This is the basis of the higher irradiance allowed for 222 nm krypton-chloride (Kr-Cl) excimer lamps relative to today's UV-C LEDs, which are typically limited to greater than 255 nm. The rapid development of UV-C LEDs indicates a likely availability of cost-effective UV-C LEDs at less than 240 nm within a few years and 225 nm within perhaps 10 yr. If the presently available 222 nm excimer lamp emission is used in conjunction with the new 2022 ACGIH TLVs[1] which allow 1279 $J \cdot m^{-2}$ vs. 37 $J \cdot m^{-2}$ allowed with 265 nm LEDs, then the attainable eACH with UV irradiated directly into the occupied space, known as direct irradiation below exposure limits (DIBEL)[2] increases from 1.6 eACH to 55 eACH. Generally, the 3× enhanced spherical fluence enabled by optical tailoring of the intensity distribution from a small LED is not available with much larger excimer sources.

However, a more efficacious and cost-effective technology than DIBEL is available today using UV-C irradiated into an unoccupied space, for example an unoccupied lavatory or galley or aisle, with reliable and redundant sensors and controls to ensure that the space is unoccupied whenever the UV irradiance exceeds the EL. With reliable sensors and controls the irradiance is allowed to greatly exceed the EL, limited only by the output of the available UV-C light source and possible long-term degradation of materials under UV-C irradiation. Commercially available UV-C systems today are capable of 30–120 eACH without significant degradation of cabin materials. This will likely increase by factors of several within a few years. When the UV-C irradiation is physically limited to a subset of the space, like the aisle or lavatory, the air in that space may be rapidly disinfected with very high UV-C irradiance, and then that disinfected air (e.g., from the aisle) is beneficially diffused elsewhere by the cabin ventilation and convection, such as to the occupied seats adjacent to the irradiated aisle. In a condition known as "well-mixed air," which is typical in most spaces with high ventilation rates, the air may be assumed to be uniformly disinfected throughout the irradiated volume (e.g., the cabin). This assumption has been validated in numerous UR-UVGI experiments in terrestrial spaces where the intense UV-C irradiates only the space above the heads of occupants, but the entire space is determined to be disinfected by the mixing of the upper room air with the entire room air.[24] The airflow from ventilation in a typical aircraft cabin is also known to create mixing of the air throughout the cabin via turbulence and eddy currents, even though the

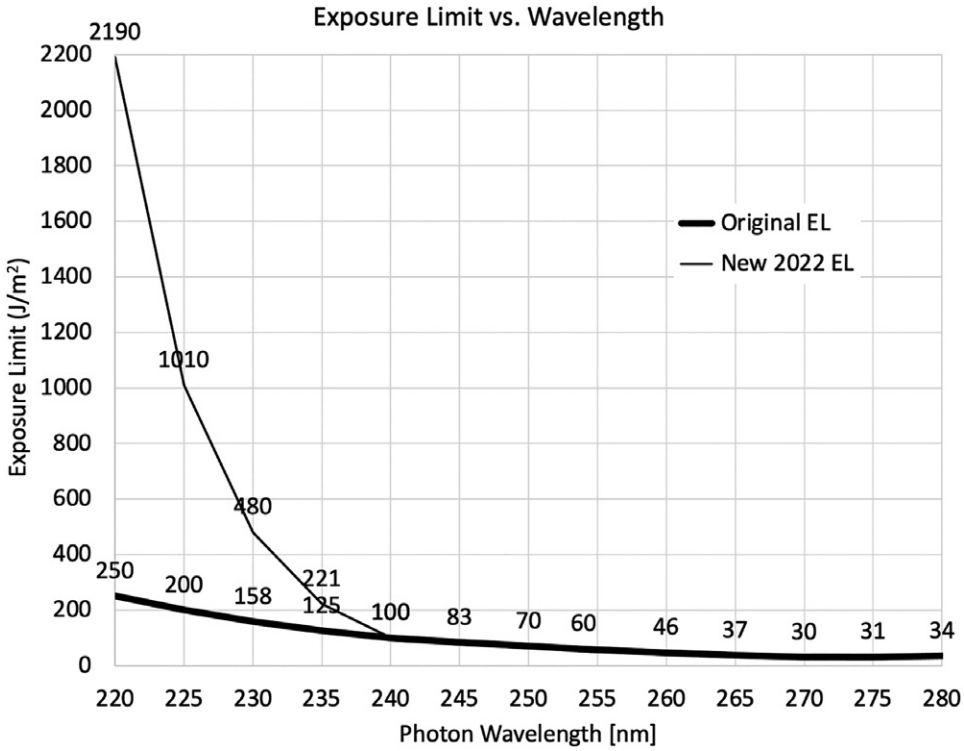

Fig. 3. Exposure limit ($J \cdot m^{-2}$) vs. UV-C wavelength (nm).

nominal direction of the airflow might be from the ceiling to the floor.[58]

In conventional UR-UVGI with mercury lamps, the UV-C has extreme spatial gradients of very high UV-C irradiance in the upper room, which result in diminishing returns of disinfection, effectively wasting a large portion of the UV-C emission. In contrast, the relatively low power and good optical beam control enabled by UV-C LEDs enables avoiding the extreme spatial gradients of very high irradiance and the resulting diminishing returns. For the case of an array of UV-C LED spot beams [e.g., having a full-width at half-max (FWHM) beam width of approximately 20° or less] spaced along the full extent of the unoccupied aisle in the cabin, with well-mixed air, and avoiding the diminishing returns of wasted high-irradiance zones, the entire emitted flux from all of the UV-C LEDs throughout the cabin may be averaged over the entire volume of air in the cabin to estimate eACH contributed by the UV. In a typical application in a Boeing 737 cabin, having an air volume of approximately 184 m^3, there may be 30 individual UV-C LEDs each emitting 150 mW (0.15 W) into spot beams along the length of the aisle, delivering a total UV-C flux of 4500 mW. Then the volume-averaged UV-C irradiance in the cabin is 24.5 $mW \cdot m^{-3}$. In a well-mixed volume of air (as in the aircraft cabin), a volume-averaged UV-C irradiance of 13–17 $mW \cdot m^{-3}$ has been shown to result in eACH of 16–24/h.[38]

This design rule whereby the expected eACH in a well-mixed space is proportional to the average UV-C power density has become a standard guideline for designing UR-UVGI air disinfection systems. Thereby, it is expected that a delivery of 24.5 $mW \cdot m^{-3}$ will result in approximately 45 eACH. Including an engineering margin to account for nonuniformities and optical efficiencies relative to the estimated 45 eACH, an actual eACH of 30 may be considered to be a baseline example of the expected UV disinfection efficacy in a commercial aircraft cabin. That baseline may be exceeded by 2–4 times by increasing the UV-C emitted from each LED, and/or by increasing the number of LEDs in the aisle by 2–4 times, so that eACH may be increased to 60–120, and even up to 200 by leveraging available options with this technology. The ACH_{UV} values estimated above for UV-C systems have not yet been experimentally validated in aircraft cabins, but estimates with a similar product have previously been validated by a certified testing lab using SARS-CoV-2 aerosolized virus in a room-sized test chamber.

As discussed above, when UV disinfection is added to the aircraft ventilation, the steady state concentration of airborne pathogens is reduced by the factor ρ from Eq. 33, repeated here:

$$\rho = \frac{ACH_{vent}}{ACH_{vent} + ACH_{UV}} \qquad \text{Eq. 33}$$

Exemplary results of Eq. 33 are presented in Table XII. The ACH_{vent} values of 15 and 30 represent a typical range while cruising, and 5 ACH_{vent} may represent an approximation while on the ground. The ACH_{UV} values are all attainable with present technology, depending on the wavelength of UV and the spacing of the UV emitters throughout the cabin. It indicates that the residual airborne pathogen concentration following airborne pathogen removal by the aircraft ventilation system may be further reduced by 33–89% while cruising, and by up to 96% while grounded. The objective of this work is to quantify the extent to which the device as installed effectively mitigates the unmanaged residual risk leftover by the ventilation system (i.e., % reduction in risk of infection or death). The formalism outlined in the above section using a mechanistic model of the fundamental Wells-Riley formalism is taken from Peng,[43] which provides a link to an Excel calculator developed by Prof. Jose L. Jimenez and Dr. Zhe Peng, Department of Chemistry & CIRES, University of Colorado-Boulder, along with a team of more than 20 other contributing experts.[29] The results presented below are derived from that Excel calculator, which enables "what if" scenarios by varying any of the input variables found in Eq. 15, repeated here:

$$PAX_{flight,inf} = N_{PAX}{}^2 \times \%_{pop,ill,day} \times \%_{fly} \times E_{p0} \times B_o \times \frac{r_{ss} \times r_E \times r_B \times f_e \times f_i \times D}{V \times ACH_{tot}} \qquad \text{Eq. 15}$$

Table XIX is excerpted from results using the UC-Boulder Excel calculator, showing only those rows of the calculator that are of interest in this study. User inputs characterize the Boeing 737 cabin, assuming $ACH_{vent} = 30$, $N = 162$ passengers, D_{cruise} = 2.5-h cruising time, 7,530,000 flights/year, 10% mask wearing of 50% effective surgical masks, and the conservative values for r_B and r_E. The first column of estimated results in Table XIX shows the baseline result of 6736 annual deaths from transmission of SARS-CoV-2 while cruising. This total of 6736 is slightly different from the 6751 calculated analytically above due to slight nonlinearities in the Excel calculator vs. the linear approximation of Eq. 15 of this document. This is the residual risk of infection with all of the mitigation factors in the Swiss Cheese model (including $ACH_{vent} = 30$ but excluding UV-C) in place over the period March 2022 through March 2023.

The second results column augments the aircraft ventilation of 30 ACH with 120 eACH from the UV-C. As expected, since ACH_{tot} has been increased by 5× above that of the ventilation alone, the estimated number of annual deaths is reduced by 77% (not exactly 80%, again displaying a slight nonlinearity in the formulas used in the Excel calculator).

The third results column augments the aircraft ventilation of 30 ACH with 100% adherence to wearing surgical masks, resulting in a 72% reduction in deaths. Interestingly, this 72% reduction, which requires a reluctant public to comply with 100% mask wearing, is comparable to the 77% reduction with UV-C that requires no active cooperation from the passengers, imposes no discomfort, and, as will be shown later, poses essentially no health risk to crew and passengers.

The fourth results column is an ideal situation, with the UV-C system operating and 100% passenger compliance in wearing N95 masks. The resulting 99.8% reduction to only 16

Table XIX. Results from UC-Boulder Excel Calculator for Various Combinations of UV and Mask Wearing as Infection Risk Mitigations for COVID-19.

ENVIRONMENTAL PARAMETERS AND RESULTS FOR BOEING 737 WHILE CRUISING						WHILE DE-ICING ON 3% OF FLIGHTS		
	EXAMPLES							
PARAMETER OR RESULT	**1**	**2**	**3**	**4**	**5**	**6**	**7**	**8**
ACH aircraft ventilation (/h)	30	30	30	30	30	5	0	5
UV-C eACH (/h)	0	120	0	120	120	0	0	120
ACH_{tot} (/h)	30	150	30	150	150	5	0	125
Masks	actual		Surgical	N95 All	N95 solo			
Duration of event, D (min)	150	150	150	150	150	60	60	60
Number of flights/yr	7.5.E+06	7.5.E+06	7.5.E+06	7.5.E+06	7.5.E+06	2.3.E+05	2.3.E+05	2.3.E+05
Total PAX, N	162	162	162	162	162	162	162	162
Basic Quanta exhale rate, E (q/h)	18.6	18.6	18.6	18.6	18.6	18.6	18.6	18.6
E enhancement due to activity	3.0	3.0	3.0	3.0	3.0	3.0	3.0	3.0
Exhalation mask efficiency, $f_e = f$	50%	0%	50%	90%	0%	50%	50%	50%
Inhalation mask efficiency, $f_i = f$	50%	0%	50%	90%	90%	50%	50%	50%
Fraction of people w/ masks	10%	0%	100%	100%	100%	10%	10%	10%
Probability of being infective, h_{inf}	0.055%	0.055%	0.055%	0.055%	0.055%	0.055%	0.055%	0.055%
Death rate	1.0%	1.0%	1.0%	1.0%	1.0%	1.0%	1.0%	1.0%
No. of deaths annually	6736	1549	1870	16	155	984	3919	50
Reduction in deaths	-	77%	72%	99.8%	98%			99%

PAX: passengers.

deaths/year provides an insight that zero deaths/year may be unrealistic in the face of deadly airborne diseases, but the potential risk reduction with UV disinfection is significant.

The fifth results column indicates that even if no other passengers are wearing masks, any given passenger who chooses to wear an N95 mask can reduce their risk of infection and death by 98% if the UV-C system is operating. The percentage reductions in deaths with the application of UV-C and/or masks will be the same for the 60-min ground portion of each flight.

The sixth through eighth columns demonstrate the worst-case scenario for risk of airborne infections aboard the aircraft—when the aircraft is on the ground, being de-iced with little or no ventilation in the cabin, typically at the peak of cold, flu, and COVID seasons during winter. The sixth column if $ACH_{vent} = 5$ (which is higher than the actual near-zero ventilation during de-icing) results in 984 deaths/year due to transmission of SARS-CoV-2 during de-icing. The seventh column assumes the more accurate $ACH_{vent} = 0$ during de-icing, resulting in 3919 deaths/year due to transmission of SARS-CoV-2 during those few flights requiring de-icing. This is a tremendous toll from a relatively few flights where de-icing is required. The eighth column indicates that the use of UV-C during de-icing potentially eliminates 99% of those deaths that are due to zero ACH cabin ventilation, reducing the toll to just 50 deaths/year.

While Table XII pertains to SARS-CoV-2, the relative reduction in deaths/year expected from application of UV-C air disinfection is the same for Influenza A, although the absolute values are lower for Influenza A.

If eACH is less than 120, then the relative reductions in deaths/year in Table XIX will be less. For example, if eACH = 30, then the second results column with ventilation = 30 ACH and eACH = 30 from the UV-C, the reduction in deaths decreases from 77 to 43%. The results of Table XIX above can be visualized in **Fig. 4** using the pictorial representation of the ICAO (International Civil Aviation Organization) Aviation Multi-Layered Disease Defense Strategy (known as the Swiss Cheese Model).

In Fig. 4 (top), the broad red arrow from the left indicates an extremely large risk (much greater than 8100 deaths) that would accrue without the benefit of the 30 ACH of cabin ventilation. When the broad red arrow passes through the mitigation provided by a low incidence of mask wearing, the risk is insignificantly abated any further. But when the broad red arrow encounters the mitigation layer (cheese slice) pertaining to 30 ACH aircraft ventilation, the risk is greatly reduced to the present level of unmitigated risk at 8100 deaths/year due to onboard transmission of airborne diseases (COVID-19 plus influenza). In Fig. 4 (bottom), the broad red arrow from the left encounters the mitigation layer pertaining to 30 ACH ventilation, reducing the risk to the present level of unmitigated risk at 8100 deaths per year, and then the contribution of 120 eACH from UV-C at the far right further reduces the residual risk by another 77%.

Of the estimated 8000 combined annual deaths due to transmission of SARS-CoV-2 and Influenza A aboard U.S. commercial aircraft, approximately 43–77% of those deaths may be avoided by supplementing the aircraft ventilation with UV-C, providing eACH equal to 30–120. Of the estimated $2.8 billion annual U.S. economic burden due to the transmission of Influenza A and $34.3 billion due to transmission of SARS-CoV-2 (for 12 mo ending March 2023) aboard U.S. commercial aircraft, approximately 43–77% of that, or $1.2–$2.2 billion/year (Influenza A) and $14.8–$26.5 billion/year (COVID-19) could be saved by supplementing the aircraft ventilation with UV-C, providing eACH = 30–120.

POTENTIAL SAFETY RISKS ASSOCIATED WITH EXPOSURE TO THE UV-C DEVICE

Repeated exposure to high doses of light of any wavelength can pose a risk to humans, particularly to skin and eye tissue. In fact, repeated exposure to high doses of visible or infrared (IR) light, as

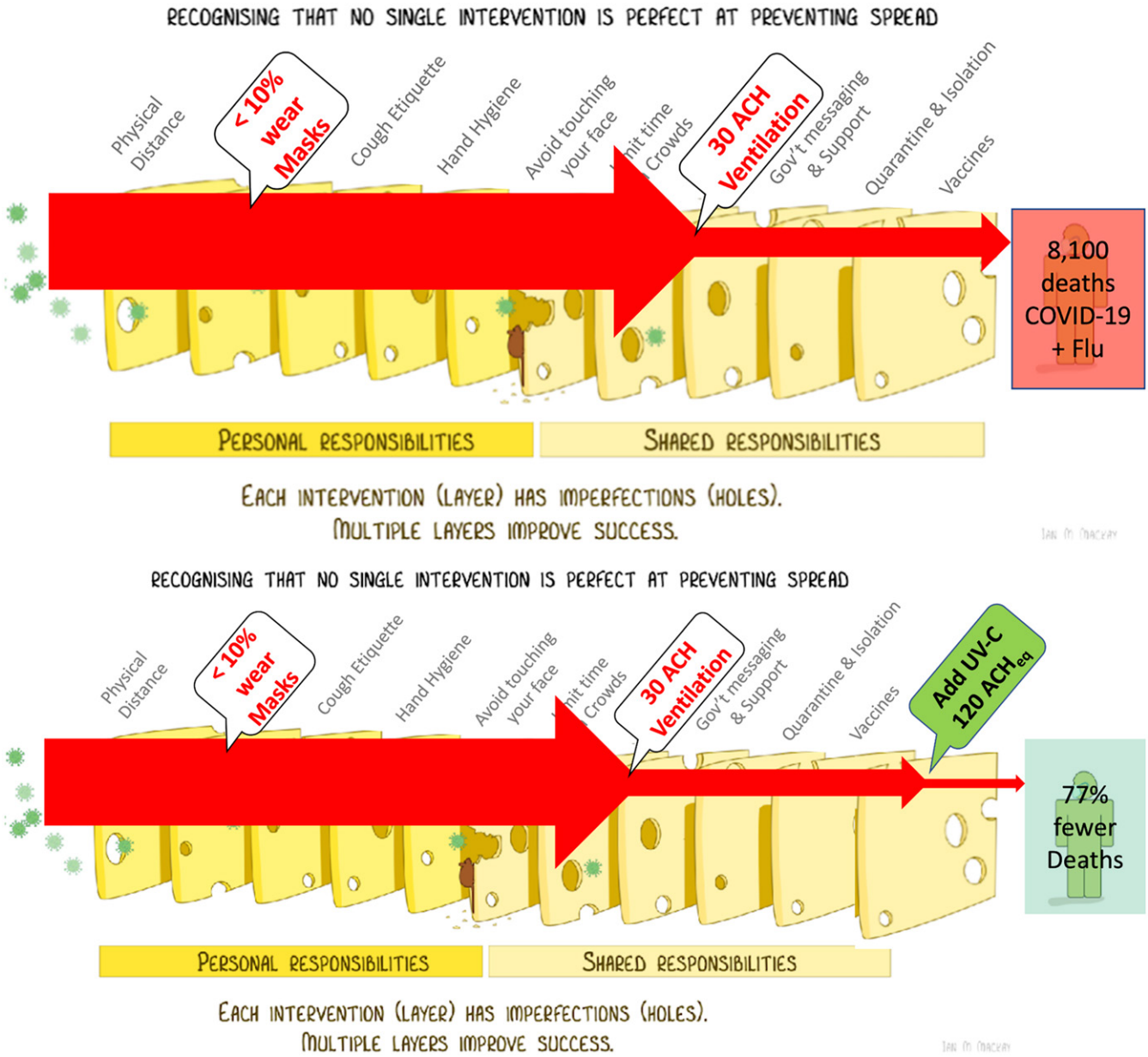

Fig. 4. ICAO Aviation Multi-Layered Disease Defense Strategy. Top: without UV-C air disinfection layer added. Bottom: with UV-C air disinfection layer added.

well as UV light, can pose risks to humans. The allowable EL (TLV) below which harm to eyes and skin is avoided is a strong function of the wavelength of the light. For any given wavelength of light (UV, visible, or IR), it is thus important to define the daily dose below which there is no expectation of photobiological harm from repeated exposure, or exposures, below the EL.[2,52] The recently emerging combination of low output power, point source optical emission of UV-C LEDs enabling optical beam control, solid-state sensors and controls for UV-C LEDs, revised guidelines for increased EL for shorter UV-C wavelengths, and improved methods for inactivation of pathogens have enabled the development of DIBEL technology, wherein the UV irradiance is maintained below the allowed EL at all locations in the space that can be occupied.[2] However, as estimated above, the theoretical upper limit of eACH is approximately 5 for 265 nm LEDs enhanced with optical beam tailoring, or 55 for optically unenhanced excimer 222 nm lamps, reduced effectively to approximately 25–30, accounting for spatial nonuniformities. While 5–30 eACH may be sufficient for most terrestrial applications, the relatively low eACH values provided by presently available DIBEL technologies are not sufficient to increase the total ACH aboard an aircraft by the at least two to five times required to substantially reduce the risk of airborne disease transmission. With the eventual potential advent of UV-C LEDs at wavelengths below 235 nm, the combination of very high allowable EL, the three times enhancement of UV-C fluence with optical tailoring enabled by the very small size of LEDs, the relatively low cost and the long life of UV-C LEDs, direct irradiation onto occupants (DIBEL) may well become the preferred future technology within aircraft cabins. Although DIBEL protocols may eventually be engineered to

irradiate occupants directly with eACH much greater than 30, providing such high eACH values in an aircraft cabin is not presently possible at affordable cost with DIBEL. Rather, present technology limitations require careful optical design with small UV-C LEDs to provide very high UV-C irradiance into unoccupied zones of the cabin (e.g., the aisle and lavatories) along with occupancy sensors and controls to virtually eliminate the possibility of UV-C overexposure to occupants in the cabin.

In the rare event of UV-C overexposure the risk of skin or eye damage may be either acute or chronic, or both. Acute damage may result from a one-time overexposure that greatly exceeds the allowed EL for an 8-h period. The damage repairs itself within 1–2 d and is not cumulative. The two acute risks, erythema and photokeratitis, and the chronic risk, that of non-melanoma skin cancer, are discussed below.

POTENTIAL SIDE EFFECTS OF UV-C RADIATION

Erythema and Photokeratitis

The very aspect (phototoxicity) that makes UV-C radiation an effective germicidal agent also is responsible for the unwanted side effects of erythema (reddening of the skin) and photokeratitis ("welder's flash" or "snow-blindness"). Overexposure to UV-C radiation can produce these unwanted side effects from a mild irritation of the skin and eyes to a rather painful case of photokeratitis. These effects are fortunately transient, as only superficial cells of the eye, the corneal epithelium, and the most superficial layer of the skin, the superficial epidermis, are significantly affected. Normal daily turnover of these cells soon erases the signs and symptoms of these effects. Radiant energy in the UV-C band has very shallow penetration depths in biological tissue, which accounts for the superficial nature of any injury to the skin and eyes from excessive exposure and minimum risk of delayed effects.[51]

As the outer (dead tissue) layer of the skin, the stratum corneum, is highly absorbing in the UV-C, only small traces of UV-C incident onto the skin may penetrate to the germinative (basal) layer of the epidermis.[51]

> *The classic studies of Hausser and Vahle showed that with increasing doses of 254 nm radiation above 1 minimal erythema dose (MED, smallest dose of UV-C radiation that can produce visible redness (erythema)), the level of redness hardly increased, even at doses 10-fold above the exposure associated with the just-perceptible redness. This was in sharp contrast to the rapid increase in redness with 313 nm irradiation (UV-B, which is the range from 280 nm through 315 nm), where severe erythema and blistering occurred at doses only 20% above those resulting in just perceptible erythema. This has been interpreted to be related to the penetration depth of the UV light. From these observations, some photodermatologists have argued that UV skin carcinogenesis is not a realistic risk from germicidal (UV-C) lamps, since only a small amount of radiation from the 254 nm line (that comprises over 90% of the radiation from a low-pressure mercury discharge lamp) reaches the germinative layer of the epidermis.*[28]

In other words, even when the EL is exceeded enough to cause reddening of the skin, a further 10 times increase in a 254-nm dose hardly increases the level of reddening, suggesting that an extreme overdose of 254-nm UV-C well above the EL still produces only minor reddening, with no long-term impact.

A radiant exposure of approximately 100 $J \cdot m^{-2}$ at 254 nm will produce photokeratitis and photoconjunctivitis (sometimes referred to as photokeratoconjuctivitis, "welders' flash," "arc eye," or "snow blindness").[5,28,51] The surface epithelial cells that are damaged from UV-C exposure are normally sloughed off overnight—certainly within 48 h.[51] This onset of 100 $J \cdot m^{-2}$ for production of photokeratitis or photoconjunctivitis is almost two times higher than the EL, which equals 60 $J \cdot m^{-2}$ at 254 nm, indicating a significant safety margin built into the EL.

Non-Melanoma Skin Cancer

The 2020 International Commission on Illumination (CIE) report 187, "UV-C Photocarcinogenesis Risks from Germicidal Lamps", has explored in depth the question of the potential for skin carcinogenesis (cancer) from UV-C light (photocarcinogenesis). This report clearly demonstrates that the risk is exceedingly small.[51] The CIE report acknowledges that "although experimental studies in animal models demonstrate that tumours are readily produced from UV-B (280–315 nm) exposures, this is not the case for UV-C (200–280 nm) exposures. Relatively high doses of UV-C irradiation were required to produce tumours in rodent models." Specifically, the CIE report references Sterenborg[53] for the tumorogensis in hairless mice due to 254-nm UV-C irradiation, which indicates in Figs. 5 and 7 of that reference that tumors having 0.7–1 mm diameter appear with 63% prevalence after 300 d of daily exposure to 230 $J \cdot m^{-2}$, and with 1% prevalence after 150 d. The test dose of 230 $J \cdot m^{-2}$ is approximately four times the allowed daily exposure limit of 60 $J \cdot m^{-2}$ at 254 nm.

Furthermore, the reason that malignant melanoma skin cancers are not presently of concern is summarized in the excerpt below from the International Commission on Non-Ionizing Radiation Protection (ICNIRP) 2004.[27]

> *For basal cell carcinoma and malignant melanoma, neither the wavelengths involved nor the exposure pattern that results in risk have been established with certainty; whereas for squamous cell carcinoma, UVB, and probably UVA, are implicated and the major risk factors seem to be cumulative lifetime exposure to UV radiation and a poor tanning response.*

The conclusion of that 2004 ICNIRP publication is confirmed in a recent 2021 review by Forbes[25]:

> *As indicated in its name, the "CIE Non-Melanoma Skin Cancer Action Spectrum" (CIENMSC) makes no*

prediction for melanomas, since those tumor types are rarely observed or diagnosed in UV–exposed hairless mice. There are currently no reliable animal models or data available for photocarcinogenesis action spectrum determination for malignant melanoma or basal cell carcinomas.

Since current rodent models are not prone to melanoma, it is difficult to determine the causality of UV-C for this malignancy with the current animal models. Additional research is needed to determine the photocarcinogenesis action spectrum for melanoma in the UV-C range.

The CIE 187 report states: "*Known side effects of overexposure to UV-C radiation include transient corneal and conjunctival irritation (photo-keratoconjunctivitis) and skin irritation (erythema), which disappear within a 24 to 48 hour period, not currently known to produce lasting biological damage.*"[28] The long-term incremental risk of nonmelanoma skin cancer (NMSC) when a person (e.g., crew) is exposed at the maximum allowed Exposure Limit for 8 h/d, 5 d/wk, for 20 yr is 0.37% above the risk of an unexposed person.[28] This result will be used below to calculate the estimated risk of NMSC for all crewmembers throughout their careers with UV-C installed aboard all aircraft.

Estimated annual statistics related to skin cancer in the United States are summarized below for NMSC and melanoma.[3,4,49]

NMSC.

- 3.6 million cases of basal cell carcinoma (BCC) and 1.8 million cases of squamous cell carcinoma (SCC) diagnosed per year.
- The annual cost of treating NMSC is $4.8 billion, approximately $900 per case.
- One in five Americans will develop skin cancer in their lifetime.
- It is thought that approximately 2000 people in the United States die each year from NMSC.

Melanoma.

- 186,680 cases diagnosed per year.
- 7990 deaths per year.
- The annual treatment cost is $3.3 billion, approximately $18,000 per case.

Squamous cell photocarcinogenesis requires the germinative layer of the epidermis to be affected, as that layer has the long-term "memory" for the skin. The real risk of UV photocarcinogenesis at 254 nm is extremely small, primarily because of the shallow penetration of this wavelength of light to the basal layer of the epithelium. The strong attenuation by the stratum corneum and epidermis above the basal layer are accounted for in the action spectrum for squamous cell carcinogenesis. The penetration to the basal layer of the epidermis becomes an insignificant value at 254 nm.[51,52] Although the mortality rate from NMSC is extremely low, there is an established correlation (but not causality) between NMSC and later development of melanoma, especially if the NMSC is SCC. So, the burden of deaths and cost of care for NMSC might need to be adjusted for that possibility, although the necessary statistics have not been found by the authors of this work.

There were enhanced risks (hazard ratio, HR, greater than 1) of other cancers following NMSC (including SCC and BCC) as follows:

- For all other cancers, HR = 1.40 (95% confidence interval, CI, 1.15, 1.71) after BCC, and HR = 1.18 (95% CI 0.95, 1.46) after SCC;
- For melanoma, HR = 3.28 (95% CI 1.66, 6.51) after BCC, and HR = 3.62 (95% CI 1.85, 7.11) after SCC;
- For prostate cancer, HR = 1.64 (95% CI 1.10, 2.46) after BCC.

The hazard ratio, as used above, is the ratio of the hazard rates corresponding to the conditions characterized by two distinct levels of a treatment variable of interest. The HRs are relative to a baseline of 3584 participants with controls adjusted for age, sex, cigarette smoking history, sun exposure factors, and family history of skin cancer. The standardized mortality ratio is the ratio of observed deaths in the study group to expected deaths in the general population.[13]

RISK REDUCTION DUE TO UV-C

Of the estimated 8000 combined annual deaths due to transmission of SARS-CoV-2 and Influenza A aboard U.S. commercial aircraft, approximately 43–77% of those deaths may be avoided by supplementing the aircraft ventilation with UV-C, providing eACH = 30–120. Of the estimated $2.8 billion annual U.S. economic burden due to transmission of Influenza A and $34.3 billion due to transmission of SARS-CoV-2 (for 12 mo ending March 2023) aboard U.S. commercial aircraft, approximately 43–77% of that, or $1.2–$2.2 billion/year (Influenza A) and $14.8–$26.5 billion/year (COVID-19) could be saved by supplementing the aircraft ventilation with UV-C, providing eACH = 30–120.

Comparative Risk Associated with Exposure to UV-C

According to the Recommended Practice (RP) for UV Germicidal Irradiation (UVGI) published by the American National Standards Institute (ANSI) and the Illuminating Engineering Society (IES), ANSI/IES RP-44-21, the current daily safety limit of 254 nm UV-C for 8 h is 60 $J \cdot m^{-2}$, whereas less than 10 min of summer sun exposure at a UV Index equal to 10 can deliver the equivalent limiting daily safety dose because of its much more penetrating UV-A and UV-B.

Extent to Which the Infection Risk Reduction Due to UV-C Outweighs the Potential Safety Risks Associated with UV-C Exposure

To emphasize this comparison, it must be realized that the UV-C irradiation level in the aircraft cabin is designed to be well below the daily allowed EL pertaining to the wavelength of

UV-C applied. For any occupant in the aircraft cabin to experience a daily exposure equal to or exceeding the EL, the sensors and controls of the UV-C disinfection system would have to either be: 1) improperly designed, 2) improperly installed, or 3) to have failed during operation. Professional installation, including UV measurements at critical locations throughout the cabin, will ensure safety relative to 1 and 2, and the inclusion of triply redundant sensors makes the probability of 3 extremely low. The RP-44-21 statement above suggests that only in the highly improbable event of an improper installation or failure of a triply redundant sensor system will any occupant be at any risk of receiving UV exposure comparable to or exceeding 10 min of sun exposure.

The greatest uncertainty in the risk-benefit analysis in this report is the quantification of the probability of improper installation of the UV-C system or a failure of the triply redundant sensors and controls. It is not possible to accurately predict those probabilities even within a factor of 10, whereas most other quantities and statistics in this report are generally known within a factor of two or less. Thus, the best one can do at this time is to make an order-of-magnitude best estimate of the risk of UV-C overexposure, calculate the resulting risk/benefit ratio, then consider whether the resulting risk/benefit ratio would be significantly affected by modifying the estimated probability of overexposure by one or more orders of magnitude. Eventually, with better data, a quantitative sensitivity analysis may be appropriate.

A selection of seat maps can be found for various models of Boeing 737, which range from 24–37 rows (assume an average 30 rows), with six seats across in most rows:

- https://theflight.info/seat-map-boeing-737-700-southwest-airlines-best-seats-in-plane/
- https://www.aircharter.com.br/en/aircraft-guide/group/boeing-usa/boeing-737-400-800-900
- https://www.delta.com/us/en/aircraft/boeing/737-900er

Considering the vertical spot beam of UV-C that provides eACH of approximately 30 throughout the cabin, each spot beam would serve 2 rows, amounting to 15 spots along the aisle, plus a spot beam for each lavatory. Assuming 3 lavatories and 1 spot beam for each of 4 assumed galley areas, totals 22 spot beams per aircraft.

Except for the staggered rows of the Southwest Airlines layout, each UV-C spot beam might strategically be placed midway between two adjacent aisles, as shown in **Fig. 5** as circles in the aisle, so as to maximize the distance from the UV-C LED in the ceiling to the armrest on any seat adjacent to the aisle for the geometry of the spot beam. A cross-section drawing of a Boeing 737 cabin interior[10] shows that the aisle width is 0.6 m. If the UV-C LED in the spot beam were mounted directly adjacent to a row, then the lateral distance from the LED to the armrest is 0.3 m and the diameter of the spot beam at the height of the armrest would be limited to less than 0.6 m. In contrast, if the LED is midway along the 0.76 m separation of rows along the aisle, as shown in Fig. 5, then the lateral distance between

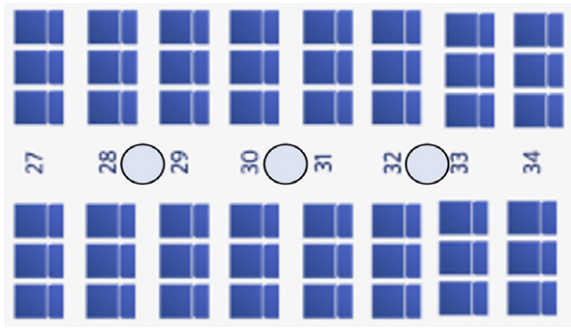

Fig. 5. Spot beam layout for B737 aircraft.

the UV-C LED and the armrest is: sqrt ($0.3^2 + 0.38^2$) = 0.48 m, so that the diameter of the spot beam may be expanded from 0.6 m to 0.96 m. This relaxed spacing allows for a greater geometric margin of safety between the armrest and the edge of the beam, as well as allowing for a greater UV flux within the beam. Thereby, safety, efficacy (eACH), and cost may all be enhanced.

In an actual prototype system, the exposure at the outer edge of the armrest is less than half the EL, and the skin or eye of a passenger would have to extend beyond the outer edge of the armrest by greater than 4″ for 8 h or more to receive an exposure equal to the EL. However, the sensors and controls are designed to turn the spot beam off if an occupant's arm extends beyond the outer edge of the armrest, so that the above scenario where an occupant receives the EL in 8 h actually requires a failure of the sensor/control system. Quantifying the probability of an occupant receiving an exposure equal to or exceeding the EL is reduced to estimating the probability that the sensor/control system of the UV-C device fails to detect an occupant beyond the outer edge of the armrest. As a conservative first estimate, one can assume that 0.01% of all devices have a defective sensor/control system which allows for an occupant whose arm extends beyond the armrest by 4″ for 8 h to receive a dose equal to the EL.

$$P_{def} \equiv \textit{Probability of a defective sensor or in any UV device, assumed to be } 0.01\%$$

In this example, each UV-C device serves 2 rows, and a total of 12 passengers, and the 4 passengers seated in the aisle seats are the only ones at risk of overexposure; thus one-third of the passengers served by each UV-C device are at risk from a defective UV-C device. Therefore, the risk that a passenger is located adjacent to a defective UV-C device is 0.003%, or 1 in 30,000 passengers. However, to receive an overexposure, the probability that a passenger keeps bare skin or eye extended at least 4″ beyond the edge of the armrest for 8 h must also be estimated. A conservatively high estimate of such might be approximately 1% of passengers.

$$P_{extend} \equiv \textit{Probability a PAX extends eye or skin at least } 4'' \textit{ beyond armrest for } 8 \textit{ hours} < 1\%$$

Then the probability that a passenger receives a dose equal to or exceeding the EL is:

$$P_{>EL} \equiv \textit{Probability that a PAX exceeds EL}$$
$$= \frac{1}{3} \times P_{def} \times P_{extend} \sim 0.00003\%$$

COMPARISON OF RISK-BENEFIT

For Acute UV-C Overexposure

From above, the estimated total number of passengers who became infected with COVID-19 annually while cruising aboard U.S. commercial aircraft over the past 12 mo is 710,000, which is approximately 0.1% of the approximately 800,000,000 annual passengers. The estimated annual number of passengers who will be infected by Influenza A, from Eq. 18, is 3,350,000, which is approximately 0.4% of the 800,000,000 annual passengers, in total, approximately 0.5% for the two diseases combined.

In this analysis, the risk of UV-C overexposure is 0.00003% and the risk of contracting COVID or Influenza A is 0.5%, so that the benefit-risk is 15,000:1. For emphasis, the intent of this study is to determine the order of magnitude of the risks and benefits of using UV-C light to mitigate the risk of airborne infection aboard commercial aircraft. The estimates of risks and benefits herein should be interpreted as having no better than a factor of 10 precision, in that precision better than that is simply not possible at this time. Later studies may provide sensitivity analyses based on varying the assumptions herein, or better precision based on more reliable assumptions and data. The 0.00003% risk of acute (one-time) overexposure, calculated in **Table XX**, may (or may not) result in a 1–2-d skin or eye irritation, with no long-term effects or risks, compared to the 15,000 times greater risk at 0.5% of contracting COVID-19 or Influenza A that persists for several days to weeks, and has a risk of hospitalization or death.

For Chronic UV-C Overexposure

There are currently no reliable animal models or data available for photocarcinogenesis action spectrum determination for malignant melanoma or basal cell carcinomas.[25] The only known long-term health risk due to chronic, occupational overexposure of UV-C is for NMSC, which is quantified in the following excerpt from the CIE Technical Report 187.[28]

> *Using the best available information, a lifetime exposure risk was calculated … which showed that an accumulated daily exposure to 254 nm radiation at the ACGIH/ICNIRP threshold limit value (TLV) (i.e., 6 mJ·cm^{-2} (3 mJ·cm^{-2} effective), received over eight h) for five days a week, over 20 years, would increase the risk of non-melanoma skin cancer by a factor of about 0.37%.*

Such long-term exposure is most likely for the flight attendants (assuming UV-C is not installed in the cockpit) rather than for passengers. As in the calculations above for acute overexposure, a chronic overexposure can only occur if a UV-C device is improperly installed, or the sensor/control system is defective. Improper installation should be avoided by measuring the UV-C output distribution upon installation, and periodically thereafter. A conservatively high probability of a defective sensor/control system (triply-redundant) in a UV-C device was estimated above to be 0.01%. If a flight attendant is seated adjacent to a defective UV-C device on a given flight, then an acute overexposure is a possibility as analyzed above. However, for a chronic overexposure to occur, that same flight attendant would have to be seated adjacent to a defective UV-C device (0.01% probability on each flight) and have skin or eye extended at least 4″ beyond the outer edge of the armrest (1% probability) constantly for nearly every flight for 20 yr. There appears to be virtually no possibility of any individual aboard an aircraft receiving a long-term chronic dose at or above the EL for 8 h/d, 5 d/wk, for 20 yr. There appears to be virtually no scenario for any occupant aboard an aircraft equipped with a UV-C device designed below the EL to receive a chronic, occupational dose of UV-C sufficient to increase the risk of NMSC if the device is installed properly and monitored periodically thereafter.

A very unlikely scenario that could result in chronic, occupational overexposure would require that a given flight attendant would be seated in the same seat on the same aircraft in which a defective UV-C device were allowed to operate without detection and correction of the defect for 20 yr and have skin or an eye extended at least 4″ beyond the outer edge of the armrest (1% probability) constantly for nearly every flight for 20 yr. In that extremely unlikely event, a flight attendant with a 20-yr flying career would have a 1% × 0.01% = 0.0001% probability of chronic overexposure (1 in 100,000 flight attendants who are employed at any given time). The number of flight attendants in the United States is approximately 100,000, of which only 19% have more than 11 yr of tenure.

From these statistics, a conservatively high estimate of the number of flight attendants presently on the job who will have at least a 20-yr career is 20,000 or less. Given the above estimate in a very unlikely scenario that any given flight attendant could have a 1 in 100,000 chance of experiencing a chronic,

Table XX. Probability of Passengers Receiving a One-Time UV Exposure Above the EL.

PARAMETER	DEFINITION	VALUE
P_{def}	Probability of a defective sensor/control	0.1%
$P_{extended}$	Probability of skin or eye extended 4″ beyond edge of armrest	1%
f_{aisle}	Fraction of passengers in an aisle seat	33%
$P_{>EL}$	Probability that any given passenger exceeds the EL = P_{def} x $P_{extended}$ x f_{aisle}	3.3E-06
PAX_{Ann}	Total passengers	1,060,000,000
$PAX\text{-}Ann_{>EL}$	Total PAX receiving 1-time UV-C dose exceeding EL = PAX_{Ann} x $P_{>EL}$	3533

UV: ultra-violet; EL: exposure limit; PAX: passengers.

Table XXI. Summary of Contact Tracing Data for Onboard Transmission of SARS-CoV-2.[45]

STUDY (FIRST AUTHOR)	INVESTIGATION	PAX TO BE TRACED	PAX TRACED	INDEX CASES	SECONDARY CASES	SECONDARY CASES WITHIN 2 ROWS	PEOPLE ON BOARD	EVIDENCE LEVEL
Bae	1	287	287	6	1	0	299	High
Bae	2	202	202	3	1	-	205	High
Blomquist	1	425	79	55	5	4	2368	High
Bohmer	2	-	-	1	0	-	-	High
Burke	1	13	13	1	0	-	-	High
Chen	1	330	330	11	1	1	342	High
Choi	2	294	0	2	2	-	294	High
Draper	1	389	326	14	0	-	-	High
Eichler	1	148	148	1	2	2	149	High
Eichler	2	-	-	2	1	1	94	High
Eldin	2	-	-	1	0	-	-	High
Khanh	1	216	184	1	15	11	217	High
Murphy	1	60	48	1	13	-	61	High
Speake	1	241	-	11	11	8	241	High
High Evidence Level Totals		2605	1617	110	52	27	4270	
Stoecklin	1	13	-	1	0	-	234	Med
Eldin	1	-	-	1	1	-	-	Med
Hoehl	1	95	95	7	2	2	102	Med
Nye	1	-	-	1	3	3	-	Med
Nye	2	-	-	2	2	2	-	Med
Nye	3	-	-	3	1	1	-	Med
Nye	4	-	-	6	1	0	-	Med
Nye	5	-	-	40	3	-	-	Med
Nye	6	-	-	5	3	3	-	Med
Bohmer	1	-	-	1	0	-	-	Low
Nir-Paz	1	9	9	2	0	-	11	Low
Pavli	1	-	981	21	5	4	2334	Low
Qian	1	-	-	1	10	-	-	Low
Schwartz	1	25	25	1	0	-	350	Low
Swadi	1	84	84	2	4	4	86	Low

PAX: passengers.

occupational (20-yr) overexposure, then there is approximately a 20% chance (20,000/100,000) that one flight attendant employed today might receive a chronic overexposure over the next 20 yr. That one-fifth of a single flight attendant who accumulates a chronic overexposure 20 yr from now would then have a 0.37% increased likelihood of having an NMSC. The lifetime risk of contracting NMSC for any American is 20%.[3] Then the incremental risk of contracting NMSC from the UV-C overexposure for that one-fifth of a flight attendant is $1/5 \times 20\% \times 0.37\% = 0.016\%$. In a very unlikely scenario that could result in chronic, occupational overexposure to flight attendants, the risk of any one flight attendant contracting NMSC over a 20-yr period due to UV-C overexposure aboard the aircraft is 0.016%. That 0.016% of an NMSC case is highly treatable, at a cost of approximately $900 per treatment, or less than $1 total economic burden, with virtually no probability of even one death.

CONCLUSION OF RISK-BENEFIT ANALYSIS

By installing UV-C air disinfection aboard all U.S. commercial aircraft, one can expect to avoid at least half of the estimated 8000 annual deaths in the United States due to transmission of Influenza A and COVID-19 during a COVID outbreak aboard aircraft, or approximately 10 avoided deaths per day. The UV-C exposure risk incurred in order to avoid 4000 annual deaths is the remote (conservatively estimated) risk of 267 passengers annually receiving a one-time acute overexposure resulting in 1–2 d of skin or eye irritation, with no long-term, chronic health risk. The conservatively underestimated benefit of saving on the order of 10 lives every day must be weighed against the conservatively overestimated risk of on the order of one passenger per day having 1–2 d of skin or eye irritation. Whereas the estimated benefit is based on statistically sound data and not susceptible to large errors, the estimated risk of UV-C overexposure has been conservatively overestimated, perhaps by 100 times or more. Therefore, it may be that only on the order of one person per year might experience 1–2 d of skin or eye irritation in order to save approximately 4000 lives per year.

The risk-benefit of economic burden results in much greater than 100% return on investment annually every year following a one-time investment of on the order of $1 billion to install UV-C in every U.S. commercial aircraft. The average cost of 80,000 lives saved over a 20-yr period by UV-C air disinfection aboard aircraft is on the order of $10,000 per avoided death. Data and analysis suggest that every day that the installation of UV-C air disinfection is delayed in the U.S. commercial aircraft fleet, perhaps on the order of 10 people die unnecessarily.

Evidence of Aerosol Transmission on Aircraft

Extensive evidence of onboard transmission of 11 different airborne diseases is available.[45] The two of interest in this document, SARS-CoV-2 and H1N1 (a subtype of Influenza A) are shown in **Table XXI** and **Table XXII**. Table XXI lists 14 separate flights where onboard transmission of SARS-CoV-2 has been traced with a high evidence level, totaling 52 secondary

Table XXII. Summary of Contact Tracing Data for Onboard Transmission of H1N1 and Influenza.[45]

STUDY (FIRST AUTHOR)	INVESTIGATION	PAX TO BE TRACED	PAX TRACED	INDEX CASES	SECONDARY CASES	SECONDARY CASES WITHIN 2 ROWS	PEOPLE ON BOARD	EVIDENCE LEVEL
Baker	1	112	102	12	4	4	379	High
Han	1	114	114	1	0	-	115	High
Han	2	110	110	1	1	0	111	High
Han	3	110	110	2	7	1	112	High
Moser	1	54	53	1	38	-	54	High
Ooi	1	596	23	1	5	2	596	High
Pang	2	1846	1846	1	8	-	1854	High
Pang	1	1283	1283	1	20	-	1303	High
Young	1	278	232	6	6	1	278	High
High Evidence Level Totals	4503	3873	26	89	8	4802		
Foxwell	1	445	145	6	8	8	445	Med
Foxwell	2	293	131	1	1	1	293	Med
Kim	1	337	199	1	1	0	338	Med
Neatherlin	1	225	146	1	8	3	226	Med
Neatherlin	2	167	133	1	4	3	168	Low
Zhang	1	274	168	1	9	-	274	Low

PAX: passengers.

cases, only 27 (52%) of which were within the conventionally assumed 2 rows of infectious range, suggesting that at least 48% of the cases were transmitted by aerosols. Note that the term "secondary or 2ndry" case in the Rafferty reference is defined in the present document to be a "primary" case, i.e., a person who is infected while onboard the flight. Table XXI lists 9 separate flights where onboard transmission of H1N1 or Influenza A has been traced with a high evidence level, totaling 89 secondary cases, only 8 (9%) of which were within the conventionally assumed 2 rows of infectious range, suggesting that at least 91% of the cases were transmitted by aerosols.

Return on Investment for U.S. Air Carriers' Installation Cost for a Typical UV-C Disinfection System in Aircraft Cabins

A UV-C disinfection system is intended to significantly improve flight safety rather than to increase revenue. However, like other safety equipment, it may have a secondary revenue enhancement effect as it improves the public's confidence in flying safety. Passengers' fear of contracting COVID-19 decreased passenger revenue for U.S. air carriers from $145.44 billion in 2019 to $49.89 billion in 2020 and $86.67 billion in 2021. The difference between 2019 and the average of 2020 and 2021 passenger revenue is $77.16 billion, a 52% loss of revenue for 2 yr. The estimated cost to U.S. air carriers for fleet-wide installation of a complete UV-C disinfection system, including UV sources, sensors, controls, wiring, etc., is such that if only 1% of passengers had their confidence improved enough to fly it would cover the entire installation cost. If 20% of passengers had their confidence improved enough to fly, then passenger revenue would have increased by $14.66 billion over the installation cost. The lifespan of a typical UV-C disinfection installation is estimated to be 20 yr, and it is possible that a pandemic as disruptive as COVID-19 will occur during this time.

ACKNOWLEDGMENTS

Financial Disclosure Statement: Gary Allen, William Mills, and Diego Garcia received compensation from ADDMAN Group.

Authors and Affiliations: Gary R. Allen, Ph.D., MS, President, Gary Allen Consulting, Inc., Aurora, CO, United States; William D. Mills, Ph.D., M.D., Consultant in Aeromedical Epidemiology, Oklahoma City, OK, United States; and Diego M. Garcia, M.D., M.Sc., Adjunct Professor, Embry-Riddle Aeronautical University, Daytona Beach, FL, United States.

REFERENCES

1. ACGIH. TLV/BEI guidelines. [Accessed May 1, 2023]. Available from https://www.acgih.org/science/tlv-bei-guidelines/.
2. Allen GR, Benner KJ, Bahnfleth WP. Inactivation of pathogens in air using ultraviolet direct irradiation below exposure limits. J Res Natl Inst Stand Technol. 2022; 126:126052.
3. American Academy of Dermatology Association. Skin cancer. [Accessed May 5, 2023]. Available from https://www.aad.org/media/stats-skin-cancer.
4. American Cancer Society. Key statistics for basal and squamous cell skin cancers. 2023. [Accessed May 5, 2023]. Available from https://www.cancer.org/cancer/types/basal-and-squamous-cell-skin-cancer/about/key-statistics.html.
5. Barnard IRM, Eadie E, Wood K. Further evidence that far-UVC for disinfection is unlikely to cause erythema or pre-mutagenic DNA lesions in skin. Photodermatol Photoimmunol Photomed. 2020; 36(6):476–477.
6. Bartsch SM, Ferguson MC, McKinnell JA, O'Shea KJ, Wedlock PT, et al. The potential health care costs and resource use associated with COVID-19 in the United States. Health Aff (Millwood). 2020; 39(6): 927–935.
7. Beck SE, Wright HB, Hargy TM, Larason TC, Linden KG. Action spectra for validation of pathogen disinfection in medium-pressure ultraviolet (UV) systems. Water Res. 2015; 70:27–37.
8. Biggerstaff M, Cauchemez S, Reed C, Gambhir M, Finelli L. Estimates of the reproduction number for seasonal, pandemic, and zoonotic influenza: a systematic review of the literature. BMC Infect Dis. 2014; 14(1):480.
9. Boeing 737-400 800 900. Air charter service. 2023. [Accessed December 5, 2023]. Available from https://www.aircharterservice.co.na/aircraft-guide/group/boeing-usa/boeing-737-400-800-900.
10. Boeing 737 aircraft profile. Flight Global. 2007. [Accessed May 5, 2023]. Available from https://www.flightglobal.com/boeing-737-aircraft-profile/76702.
11. Buonanno G, Morawska L, Stabile L. Quantitative assessment of the risk of airborne transmission of SARS-CoV-2 infection: prospective and retrospective applications. Environ Int. 2020; 145:106112.
12. Bureau of Transportation Statistics. Full-year 2021 and December 2021 U.S. airline traffic data. 2022. [Accessed 17 April 2023]. Available from https://www.bts.gov/newsroom/full-year-2021-and-december-2021-us-airline-traffic-data.
13. Centers for Disease Control and Prevention. CDC archive. Lesson 3: measures of risk. Section 3: mortality frequency measures. 2012. [Accessed November 23, 2024]. Available from https://archive.cdc.gov/#/details?url=https://www.cdc.gov/csels/dsepd/ss1978/lesson3/section3.html.
14. Centers for Disease Control and Prevention. Ending isolation and precautions for people with COVID-19: interim guidance. 2022. [Accessed 17 April 2023]. Available from https://www.cdc.gov/coronavirus/2019-ncov/hcp/duration-isolation.html.
15. Centers for Disease Control and Prevention. Estimated COVID-19 burden. 2022. [Accessed 17 April 2023]. Available from https://www.cdc.gov/coronavirus/2019-ncov/cases-updates/burden.html.
16. Centers for Disease Control and Prevention. Estimated flu-related illnesses, medical visits, hospitalizations, and deaths in the United States—2019–2020 flu season. 2023. [Accessed 17 April 2023]. Available from https://www.cdc.gov/flu/about/burden/2019-2020.html.
17. Centers for Disease Control and Prevention. Key facts about influenza. 2023. [Accessed 17 April 2023]. Available from https://www.cdc.gov/flu/about/keyfacts.htm.
18. Centers for Disease Control and Prevention. National, regional, and state level outpatient illness and viral surveillance. Fluview Interact. 2023. [Accessed 17 April 2023]. Available from https://gis.cdc.gov/grasp/fluview/fluportaldashboard.html.
19. Chiu S, Chuang J, Michelson DG. Characterization of UWB channel impulse responses within the passenger cabin of a Boeing 737-200 aircraft. IEEE Trans Antenn Propag. 2010; 58(3):935–945.
20. Civil Aviation Authority Strategy & Policy Department. CAA passenger survey report 2017. Crawley, West Sussex (United Kingdom): Civil Aviation Authority; 2018.
21. Cutler DM, Summers LH. The COVID-19 pandemic and the $16 trillion virus. JAMA. 2020; 324(15):1495–1496.
22. de Courville C, Cadarette SM, Wissinger E, Alvarez FP. The economic burden of influenza among adults aged 18 to 64: a systematic literature review. Influenza Other Respir Viruses. 2022; 16(3):376–385.

23. Federal Aviation Administration. ASPM taxi times: standard report. [Accessed May 5, 2023]. Available from https://aspm.faa.gov/aspmhelp/index/ASPM_Taxi_Times__Standard_Report.html.
24. First MW, Nardell EA, Chaisson W, Riley RL. Part I: basic principles. In: Guidelines for the application of upper-room ultraviolet germicidal irradiation for preventing transmission of airborne contagion. Transactions-American Society of Heating Refrigerating and Air Conditioning Engineers; Jan. 23, 1999; Chicago, IL, United States. Peachtree Corners (GA): ASHRAE; 1999; 105:869–876.
25. Forbes PD, Cole CA, deGruijl F. Origins and evolution of photocarcinogenesis action spectra, including germicidal UVC†. Photochem Photobiol. 2021; 97(3):477–484.
26. Handler FA. Predicting inactivation of Bacillus subtilis spores exposed to broadband and solar ultraviolet light. Environ Eng Sci. 2019; 36(6):667–680.
27. International Commission on Non-Ionizing Radiation Protection. Guidelines on limits of exposure to ultraviolet radiation of wavelengths between 180 Nm and 400 Nm (incoherent optical radiation). Health Phys. 2004; 87(2):171–86.
28. Internationale Beleuchtungskommission, editor. UV-C photocarcinogenesis risks from germicidal lamps: technical report. Vienna: CIE Central Bureau; 2010.
29. Jimenez J, Peng Z. COVID-19 aerosol transmission estimator. [Accessed May 5, 2023]. Available from https://docs.google.com/spreadsheets/d/16K1OQkLD4BjgBdO8ePj6ytf-RpPMlJ6aXFg3PrIQBbQ/edit?usp=embed_facebook.
30. Johansson MA, Quandelacy TM, Kada S, Prasad PV, Steele M, et al. SARS-CoV-2 transmission from people without COVID-19 symptoms. JAMA Netw Open. 2021; 4(1):e2035057.
31. Kennedy HE. Ultraviolet air and surface treatment. In: 2019 ASHRAE Handbook—HVAC applications, chapter 62. Atlanta (GA): American Society of Heating, Refrigerating and Air-conditioning Engineers; 2019:62.1–62.17.
32. Kowalski W. Ultraviolet germicidal irradiation handbook: UVGI for air and surface disinfection. Berlin (Germany): Springer; 2009:155–286.
33. Kujundzic E, Matalkah F, Howard CJ, Hernandez M, Miller SL. UV air cleaners and upper-room air ultraviolet germicidal irradiation for controlling airborne bacteria and fungal spores. J Occup Environ Hyg. 2006; 3(10):536–546.
34. Ma B, Linden YS, Gundy PM, Gerba CP, Sobsey MD, Linden KG. Inactivation of coronaviruses and Phage phi 6 from irradiation across UVC wavelengths. Environ Sci Technol Lett. 2021; 8(5):425–430.
35. Mathieu E, Ritchie H, Rodés-Guirao L, Appel C, Gavrilov D, et al. United States: coronavirus pandemic country profile. 2023. [Accessed 17 April 2023]. Available from https://ourworldindata.org/coronavirus/country/united-states.
36. Miller SL, Hernandez M, Kujundzic E, Howard C. Evaluating portable air cleaner removal efficiencies for bioaerosols. Rockville (MD): National Institute for Occupational Safety and Health; 2002.
37. Molinari N-AM, Ortega-Sanchez IR, Messonnier ML, Thompson WW, Wortley PM, et al. The annual impact of seasonal influenza in the US: measuring disease burden and costs. Vaccine. 2007; 25(27):5086–5096.
38. Mphaphlele M, Dharmadhikari AS, Jensen PA, Rudnick SN, van Reenen TH, et al. Institutional tuberculosis transmission. Controlled trial of upper room ultraviolet air disinfection: a basis for new dosing guidelines. Am J Respir Crit Care Med. 2015; 192(4):477–484.
39. National Research Council. The airliner cabin environment and the health of passengers and crew. Washington (DC): National Academies Press; 2002.
40. Our World in Data. Daily new confirmed COVID-19 cases. COVID-19 Data Explorer; 2023. [Accessed 17 April 2023]. Available from https://ourworldindata.org/covid-cases.
41. Parliamentary Office of Science and Technology. Statistical information on air passenger numbers and characteristics. London (UK): Parliamentary Office of Science & Technology; 2000.
42. Pawlyk O. It's almost impossible to get COVID-19 on an airplane, new military study suggests. Military.com, 2020. [Accessed 5 May 2023]. Available from https://www.military.com/daily-news/2020/10/15/its-almost-impossible-get-covid-19-airplane-new-military-study-suggests.html.
43. Peng Z, Rojas ALP, Kropff E, Bahnfleth W, Buonanno G, et al. Practical indicators for risk of airborne transmission in shared indoor environments and their application to COVID-19 outbreaks. Environ Sci Technol. 2022; 56(2):1125–1137.
44. Putri WCWS, Muscatello DJ, Stockwell MS, Newall AT. Economic burden of seasonal influenza in the United States. Vaccine. 2018; 36(27):3960–3966.
45. Rafferty AC, Bofkin K, Hughes W, Souter S, Hosegood I, et al. Does 2x2 airplane passenger contact tracing for infectious respiratory pathogens work? A systematic review of the evidence. PLoS One. 2023; 18(2):e0264294.
46. Richards F, Kodjamanova P, Chen X, Li N, Atanasov P, et al. Economic burden of COVID-19: a systematic review. Clinicoecon Outcomes Res. 2022; 14:293–307.
47. Riley RL, Nardell EA. Clearing the air: the theory and application of ultraviolet air disinfection. Am Rev Respir Dis. 1989; 139(5):1286–1294.
48. Rothman T. The cost of influenza disease burden in U.S. population. Int J Econ Manag Sci. 2017; 6(4):443.
49. Skin Cancer Foundation. Skin cancer facts & statistics. 2024. [Accessed November 23, 2024]. Available from https://www.skincancer.org/skin-cancer-information/skin-cancer-facts/.
50. Silcott D, Kinahan SM, Santarpia JL, Silcott B. TRANSCOM/AMC commercial aircraft cabin aerosol dispersion tests. Omaha (NE): National Strategic Research Institute; 2020.
51. Sliney D. Balancing the risk of eye irritation from UV-C with infection from bioaerosols. Photochem Photobiol. 2013; 89(4):770–776.
52. Sliney DH, Stuck BE. A need to revise human exposure limits for ultraviolet UV-C radiation†. Photochem Photobiol. 2021; 97(3):485–492.
53. Sterenborg HJCM, van der Putte SCJ, van der Leun JC. The dose response relationship of tumorigenesis by ultraviolet radiation of 254 nm. Photochem Photobiol. 1988; 47(2):245–253.
54. van Doremalen N, Bushmaker T, Morris DH, Holbrook MG, Gamble A, et al. Aerosol and surface stability of SARS-CoV-2 as compared with SARS-CoV-1. N Engl J Med. 2020; 382(16):1564–1567.
55. Walker CM, Ko G. Effect of ultraviolet germicidal irradiation on viral aerosols. Environ Sci Technol. 2007; 41(15):5460–5465.
56. Whalen JJ. Environmental control for tuberculosis: basic upper-room ultraviolet germicidal irradiation guidelines for healthcare settings. Cincinatti (OH): National Institutes of Occupational Safety and Health; 2009. Report No.: DHHS 2009-105.
57. World Bank. Total population for United States. World Development Indicators; 2023. [Accessed 17 April 2023]. Available from https://fred.stlouisfed.org/series/POPTOTUSA647NWDB.
58. Zee M, Davis AC, Clark AD, Wu T, Jones SP, et al. Computational fluid dynamics modeling of cough transport in an aircraft cabin. Sci Rep. 2021; 11(1):23329.

Aerospace Medicine and Human Performance
INFORMATION FOR AUTHORS
http: //editorialmanager.com/AMHP

These notes are provided for the convenience of authors considering preparation of a manuscript. Definitive information appears in the **Instructions For Authors** as published on the journal's website. Submissions that do not substantially conform to those instructions will be returned without review. We conform to the International Committee of Medical Journal Editors (ICMJE) Recommendations for the Conduct, Reporting, Editing and Publication of Scholarly Work in Medical Journals.

JOURNAL MISSION AND SCOPE

Aerospace Medicine and Human Performance is published monthly by the Aerospace Medical Association. The journal publishes original articles that are subject to formal peer review as well as teaching materials for health care professionals. The editor will not ordinarily review for publication work that is under consideration or has been accepted or published by another journal except as an abstract or a brief preprint.

TYPES OF PAPERS

The five types of articles specified below should be submitted through the web site and will undergo peer review. Other articles, including **Letters to the Editor**, **Book Reviews**, and teaching materials, should be submitted by e-mail to the Editorial Office. Letters to the Editor are limited to 500 words of discussion and/or criticism of scientific papers that have appeared in the journal within the past year. *If your manuscript does not fit the parameters laid out below, an exception may be granted. Please contact the Editorial Office to discuss your submission.*

Research Articles present the results of experimental or descriptive studies with suitable statistical analysis of results. They should contain an Introduction, Methods, Results and Discussion with a statement of conclusions. Such manuscripts should not exceed 6000 words with approximately 25 references.

Review Articles are scholarly reviews of the literature on important subjects within the scope of the journal. Authors considering preparation of a review should contact the Editor to ascertain the suitability of the topic. Reviews generally may not exceed 6000 words with up to 150 references, but longer reviews of exceptional quality will be considered.

Case Reports and ***Case Series*** describe interesting or unusual clinical cases or aeromedical events. They should include a short Background to provide perspective, the Presentation of the Case, and Discussion that includes reference to pertinent literature and/or review of similar cases. Such manuscripts should not exceed 3000 words with approximately 12 references.

Short Communications and ***Technical Notes*** describe new techniques or devices or interesting findings that are not suitable for statistical analysis. They should contain the same sections as a Research Article but should not exceed 3000 words with approximately 12 references.

Commentaries are brief essays that set forth opinion or perspective on relevant topics. Such manuscripts may not exceed 1000 words with approximately 10 references without tables or figures.

We also accept ***Historical Notes*** and ***Aerospace Medicine Clinic*** (formerly **You're the Flight Surgeon**) articles.

RULES FOR DETERMINING AUTHORSHIP

Each person designated as an author should have made substantial intellectual contributions as specified in the Instructions for Authors.

AI POLICY

The journal's AI policy can be found at https://www.asma.org/asma/media/AsMA/pdf-journal/AmHP-AI-Journal-Policy.pdf.

ETHICAL USE OF HUMAN SUBJECTS AND ANIMALS

The Aerospace Medical Association requires that authors adhere to specific standards for protection of human subjects and humane care and use of animals. The methods section of a manuscript must explicitly state how these standards were implemented. Details appear as specified in the Instructions for Authors.

LANGUAGE, MEASUREMENTS AND ABBREVIATIONS

The language of the journal is standard American English. Authors who are not perfectly fluent in the language should have the manuscript edited by a native speaker of English before submission. Measurements of length, weight, volume and pressure should be reported in metric units and temperatures in degrees Celsius. Abbreviations and acronyms should be used only if they improve the clarity of the document.

PREPARATION OF TABLES AND FIGURES

Tables and figures should be used strictly to advance the argument of the paper and to assess its support. Authors should plan their tables and figures to fit either one journal column (8.5 cm), 1.5 columns (12.5 cm), or the full width of the printed page (18 cm). Tables should be assigned consecutive Roman numerals in the order of their first citation in the text. Tables should not ordinarily occupy more than 20% of the space in a journal article. Figures (graphs, photographs and drawings) should be assigned consecutive Arabic numerals in the order of their first citation in the text. Line drawings of equipment are preferable to photographs. All graphics should be black & white: 1200 dpi for line art; 300 dpi for photos; 600 dpi for combination art. They must be sent electronically, preferably as high resolution TIFF or EPS files. See Documents to Download online for further instructions.

REFERENCE STYLE

The style for references is based on the National Library of Medicine (NLM) format, using citation-order, i.e., numbered in the order cited.

SELECTION AND FORMATTING OF REFERENCES

The Corresponding Author is responsible for providing complete, accurate references so that a reader can locate the original material. References must be cited in numerical order in the text, tables, and figure captions; the reference list should be created after all references have been cited. If electronic references are used, they should be readily available to the reader.

MANUSCRIPT SUBMISSION (see details online)

Files for Uploading:

1) signed cover letter; 2) abstract; 3) manuscript; 4) figures; 5) author checklist; 6) Copyright Release Form; 7) Conflict of Interest Form; 8) agreement to pay charges (Pub Cost Form) for excessive figures or tables, color, Open Access fees, and supplemental materials; 9) permissions (if applicable); 10) **FOR OPEN ACCESS ONLY:** licensing agreement.

PUBLICATION PROCEDURES

Once the Editor has accepted a manuscript, the electronic source files for text and figures (TIFF or EPS preferred) are forwarded to the publisher, the Aerospace Medical Association, for conversion to printable format and final copy-editing. Correspondence related to publication should be directed to the Managing Editor at the Association Home Office: (703) 739-2240, X101; rtrigg@asma.org.

When the paper is ready for publication, the printer places on its web site a PDF file depicting the typeset manuscript. The Corresponding Author will be notified by e-mail and is responsible for correcting any errors and for responding to any "Author Queries" (AQs).

EDITORIAL OFFICE

David Newman, AM, D.Av.Med., MBA, Ph.D., Editor-in-Chief
c/o Aerospace Medical Association
320 South Henry Street
Alexandria, VA 22314-3579
Phone: (703)739-2240 x 103; **Fax:** (703) 739-9652
E-mail: AMHPJournal@asma.org